Journal of Medicinal Chemistry

Article

Molecular Basis for the N-Terminal Bromodomain and Extra Terminal (BET) Family Selectivity of a Dual Kinase-Bromodomain Inhibitor

Anand Divakaran, Siva Kumar Talluri, Alex M. Ayoub, Neeraj Mishra, Huarui Cui, John C. Widen, Norbert Berndt, Jin-Yi Zhu, Angela S Carlson, Joseph J. Topczewski, Ernst Schönbrunn, Daniel A. Harki, and William C. K. Pomerantz

J. Med. Chem., **Just Accepted Manuscript** • DOI: 10.1021/acs.jmedchem.8b01248 • Publication Date (Web): 25 Sep 2018

Just Accepted

ACS Publications

is published by the American Chemical Society. 1155 Sixteenth Street N.W., Washington, DC 20036

Molecular Basis for the N-Terminal Bromodomain and Extra Terminal (BET) Family Selectivity of a Dual Kinase-Bromodomain Inhibitor

Anand Divakaran,[†‡] Siva K. Talluri,[§‡] Alex M. Ayoub,[§] Neeraj K. Mishra,[§] Huarui Cui,[§] John C. Widen,[†] Norbert Berndt,[#] Jin-Yi Zhu,[#] Angela S. Carlson,[§] Joseph J. Topczewski,[§] Ernst K. Schonbrunn,[#] Daniel A. Harki,[†] and William C.K. Pomerantz[‡*]*

† Department of Medicinal Chemistry, University of Minnesota, 2231 6th St SE, Minneapolis, MN 55455, United States

§ Department of Chemistry, University of Minnesota, 207 Pleasant St. SE, Minneapolis, MN 55455, United States

Drug Discovery Department, H. Lee Moffitt Cancer Center and Research Institute, 12902 Magnolia Drive, Tampa, FL 33612, United States

KEYWORDS

Epigenetics, BET Bromodomain, Inflammation, ^{19}F-NMR, Kinase-Bromodomain Inhibitor

ABSTRACT: As regulators of transcription, epigenetic proteins that interpret post-translational modifications to N-terminal histone tails are essential for maintaining cellular homeostasis. When dysregulated, 'reader' proteins become drivers of disease. In the case of bromodomains, which recognize N-ε-acetylated-lysine, selective inhibition of individual Bromodomain and Extra Terminal (BET) family bromodomains has proven challenging. We describe the >55-fold N-terminal BET bromodomain selectivity of 1,4,5-trisubstituted imidazole dual kinase-bromodomain inhibitors. Selectivity for the BRD4 N-terminal bromodomain (BRD4(1)) over its second bromodomain (BRD4(2)) arises from the displacement of ordered waters, and the conformational flexibility of Lysine-141 in BRD4(1). Cellular efficacy was demonstrated via reduction of c-Myc expression, inhibition of NF-κB signaling, and suppression of IL-8 production through potential synergistic inhibition of BRD4(1) and p38α. These dual-inhibitors provide a new scaffold for domain-selective inhibition of BRD4, the aberrant function of which plays a key role in cancer and inflammatory signaling.

Introduction

How our genetic information is manipulated and ultimately expressed as a heritable phenotype is a central question in the field of epigenetics. N-terminal modifications on conserved histone proteins are key regulators of transcription.[1,2] As such, proteins that interpret these complex modifications through molecular recognition are known to be essential for maintaining cellular homeostasis, or when dysregulated, they become drivers of disease.[3,4] Bromodomains are a subset of epigenetic 'reader' or effector domain-containing proteins, which function via binding to distinct lysine acylation states, most commonly N-ε-acetylated-lysine (K_{ac}) on histones.[5] This similar mode of molecular recognition for all 61 human bromodomains presents a significant hurdle for finding selective inhibitors as both therapeutic agents and chemical probes.[6]

One family of bromodomains with clinical relevance are the bromodomain and extra terminal (BET) proteins, BRD2, BRD3, BRD4, and testis specific BRDT, each of which contain a pair of bromodomains. Recent studies have shown divergent roles of these domains for targeting both acetylated histones and acetylated transcription factors, through the N- and C-terminal bromodomains (D1 and D2, respectively).[7] Prominent roles of the BRD4 BET bromodomains include regulation of c-Myc expression at super-enhancers,[8] and enhancement of NF-κB-mediated transcription through interactions with acetylated K310 of the κB RelA subunit.[7]

Due to the biological significance of bromodomain function in cellular proliferation and inflammatory pathways, over 20 clinical trials are underway for studying the effects of BET family inhibition as anti-cancer and anti-inflammatory therapies. Because of the high sequence identity among BET proteins, most reported inhibitors act as pan-inhibitors of BET bromodomains, such as (+)-JQ1 (**1**, Fig.1), and do not discern the function of individual bromodomains.[9] Ouyang et al. reported FL-411 (**2**, Fig.1), which is an exception to the norm in being selective for BRD4 over other BET proteins.[10] Nevertheless, the potential off-target effects, dose-limiting thrombocytopenia, and concerns over latent viral reactivation associated with pan-BET inhibition highlight the need for novel scaffolds with improved selectivity and/or potency.[11–13]

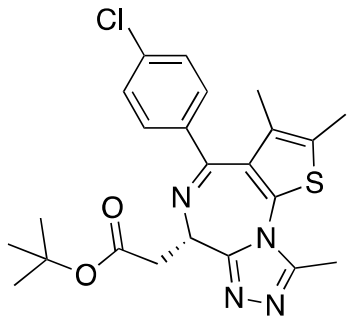

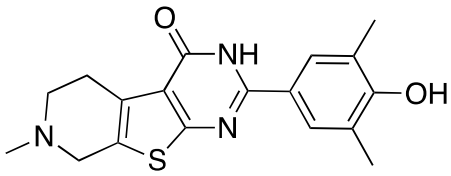

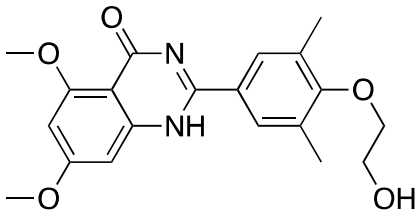

Many Pan-BET Inhibitors

(+)-JQ1 (1)
BRD4(1) K_d = 0.049 μM
BRD4(2) K_d = 0.090 μM
BRD3(1) K_d = 0.059 μM
BRD3(2) K_d = 0.082 μM
BRD2(1) K_d = 0.13 μM
BRD2(2) K_d = ND

BRD4 Inhibitors

FL-411 (2)
BRD4(1) IC_{50} = 0.47 μM
BRD4(2) IC_{50} = 0.93 μM
BRD3(1) IC_{50} = >100 μM
BRD3(2) IC_{50} = >100 μM
BRD2(1) IC_{50} = 24.6 μM
BRD2(2) IC_{50} = >100 μM

BET-D2 Inhibitors

RVX-208 (3)
BRD4(1) K_d = 1.1 μM
BRD4(2) K_d = 0.13 μM
BRD3(1) K_d = 4.0 μM
BRD3(2) K_d = 0.19 μM
BRD2(1) K_d = 5.8 μM
BRD2(2) K_d = 0.25 μM

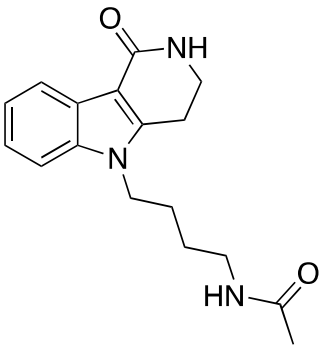

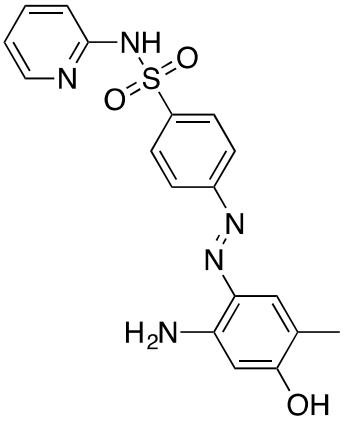

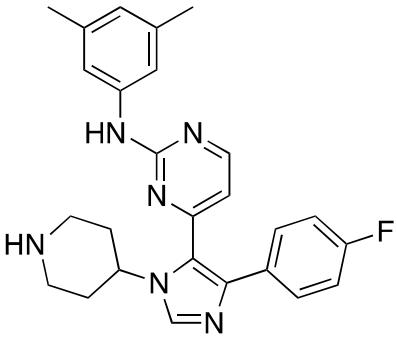

Few BET-D1 Inhibitors

Olinone (4)
BRD4(1) K_d = 3.4 μM
BRD4(2) K_d = >75 μM
BRD3(1) K_d = 3.7 μM
BRD3(2) K_d = >75 μM
BRD2(1) K_d = 8.6 μM
BRD2(2) K_d = >75 μM

MS-436 (5)
BRD4(1) K_i = < 0.085 μM
BRD4(2) K_i = 0.34 μM
BRD3(1) K_i = 0.10 μM
BRD3(2) K_i = 0.14 μM

This Work:

Compound V
BRD4(1) IC_{50} = 1.8 μM,
K_d = 1.2 μM
BRD4(2) IC_{50} = >100 μM
BRD3(1) IC_{50} = 11 μM
BRD3(2) IC_{50} = >100 μM
BRD2(1) IC_{50} = 29 μM
BRD2(2) IC_{50} = 67 μM

Figure 1: Reported BET bromodomain inhibitors and a new 1,4,5 trisubstituted imidazole, **V**.

In lieu of isoform specific inhibitors, domain selectivity among the BET family of proteins has been explored. D2-selective molecules RVX-208 (**3**, Fig.1) and -297 have allowed the study of D2-dependent processes, but have reduced efficacy mitigating BET-related transcription in

comparison to pan-BET inhibition.[14,15] Alternatively, specific deletion of only BRDT(1) in mice was sufficient to impair spermatogenesis.[16] In the case of BRD4, fluorescence recovery after photobleaching experiments identified similar levels of BRD4 displacement from chromatin between a D1 defective mutant and (+)-JQ1 (**1**) treated cells, whereas chromatin binding by a D2 defective mutant was less affected.[17] In relation to NF-κB signaling, interactions of BRD4(1) are likely more relevant for targeting transcriptional activity.[18] Although molecules MS-436 (**4**, Fig.1) and Olinone (**5**, Fig.1**)** have been reported to possess some level of D1 selectivity,[19–21] BET bromodomain research continues to be dominated by pan-BET inhibitors. Despite being potent BRD4(1) inhibitors, **4** and structural analog MS-611 are not selective for D1 over D2 in other BET proteins. In contrast, D1-selective molecule **5** is a modest inhibitor of BRD4(1) (K_d = 3.3 μM), but represents the highest level of selectivity. Alternative chemical-biology strategies like the 'bump-and-hole' approach[22,23] have considerably advanced our understanding of individual BET-bromodomain and -protein function. However, improved D1 selective inhibitors are still required to further dissect the relevant interactions of BRD4 with chromatin and acetylated transcription factors. The development of such small molecules may have significant implications for studying the roles of relevant BET proteins in transcription and the treatment of disease.

In this report we describe dual kinase-bromodomain inhibitors with the strongest affinity for BRD4(1) among BET bromodomains. While other BET bromodomain inhibitors have been reported in the literature, a notable feature of this molecule is its selectivity for the first bromodomains of BET proteins with simultaneous kinase inhibitory activity against mitogen-activated protein (MAP) kinase p38α. The atomic-level insights from structural analysis and structure-activity relationships will inform the future development of BET D1-selective

inhibitors, while optimization of this dual inhibitor should afford a useful tool compound to test synergistic effects in treating inflammation and cancer.

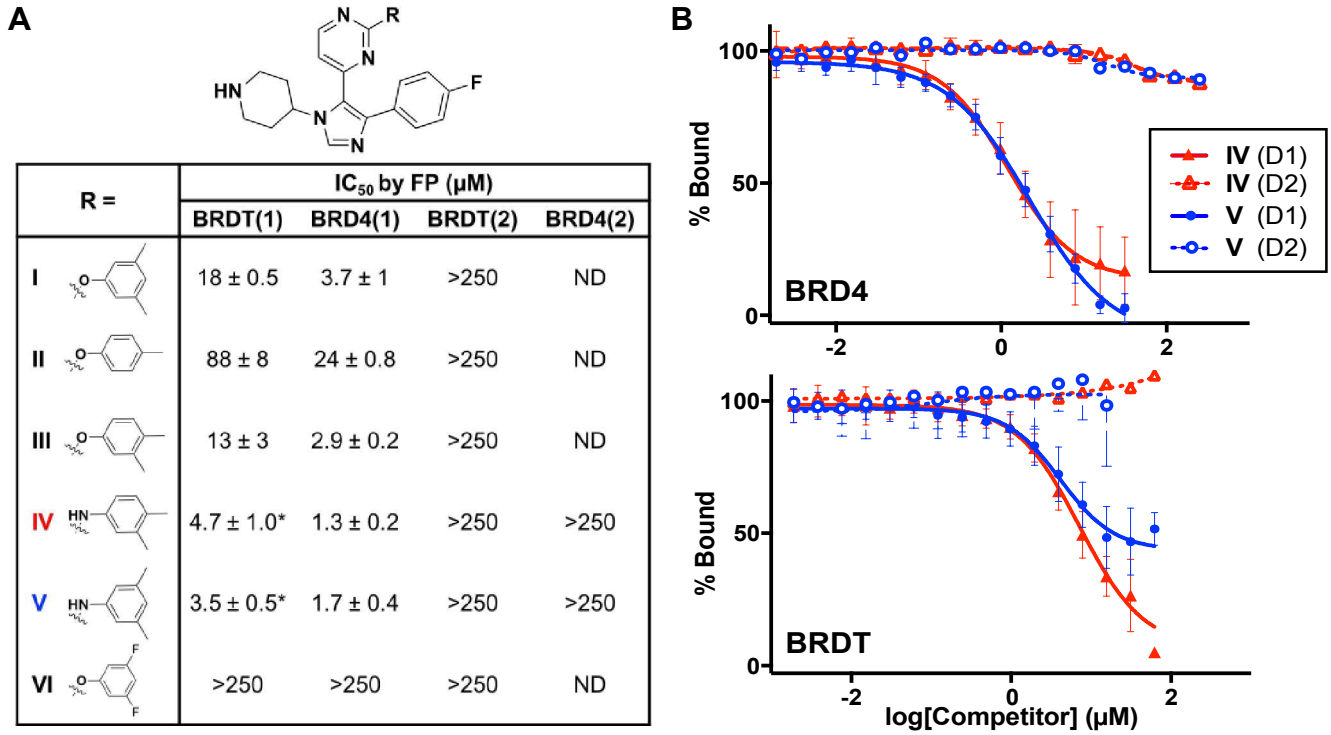

R =	IC$_{50}$ by FP (μM)			
	BRDT(1)	BRD4(1)	BRDT(2)	BRD4(2)
I	18 ± 0.5	3.7 ± 1	>250	ND
II	88 ± 8	24 ± 0.8	>250	ND
III	13 ± 3	2.9 ± 0.2	>250	ND
IV	4.7 ± 1.0*	1.3 ± 0.2	>250	>250
V	3.5 ± 0.5*	1.7 ± 0.4	>250	>250
VI	>250	>250	>250	ND

Figure 2: Competitive inhibition experiments via fluorescence anisotropy of SB-284851-BT (**I**) and analogs against BET bromodomains indicates selectivity for BET-D1s. **A**. Mean ± SEM IC$_{50}$ values of analogs determined by competitive fluorescence anisotropy assays (*indicates incomplete inhibition observed, ND = not determined). **B**. Competition binding isotherms of compounds **IV** and **V** against the first and second bromodomains of BRD4 and BRDT.

Results

The 1,4,5-trisubstituted imidazole, SB-284851-BT (**I**) and related analogs, are known p38α inhibitors and were recently discovered to bind to BET bromodomains in three separate reports using diverse libraries, including the published kinase inhibitor set library from GlaxoSmithKline. [24–26] This study tested for BET bromodomain selectivity by using a ^{19}F NMR

assay which simultaneously assessed binding to BRD4(1) and the bromodomain of BPTF.[26] SB-284851-BT was selective for BRD4(1) over BPTF in the assay and was further validated as a ligand in a thermal stability assay, differential scanning fluorimetry (DSF), and a fluorescence anisotropy (FA) assay displacing fluorescently-labeled pan-BET ligand, BI-6727, referred to here as BI-BODIPY. While our previous study identified selectivity for the BET family, we did not further evaluate selectivity within the BET family of bromodomains.

Scheme 1: Synthesis of Common Intermediate **17**

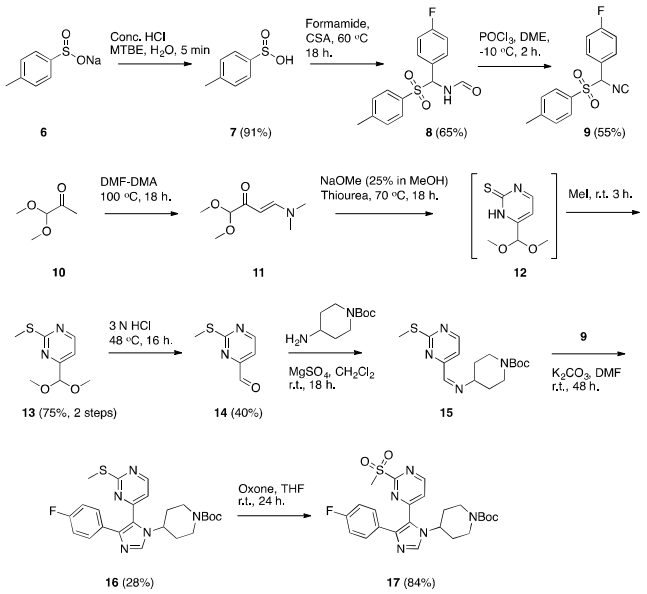

Procedure adapted from Boehm et al. and Adams et al.[27,51]

We first turned our attention to two BET bromodomains, BRDT(1) and BRD4(1). Based on significant differences in affinity arising from methyl substitution patterns on the phenyl ring of **I** for BRD4(1),[26] we synthesized several new analogs and determined their affinity to these two domains. The synthesis for SB-284851-BT (**I**) has already been established,[27] and we took advantage of a late stage intermediate (Scheme 1) for analog synthesis using a nucleophilic aromatic substitution reaction with various phenolic and anilinic derivatives (Schemes 2-4), of

which several are described here (Fig.2A). Using FA to quantify the activity of these newly synthesized compounds against both BRDT(1) and BRD4(1), we found that compound **I** binds to both domains. The observed affinity for BRD4(1) was 3-fold weaker than the previously reported data of the compound used directly from the library stock, indicating a possible discrepancy in concentration or purity. Consistent with our prior report,[26] the para-substituted analog, **II**, bound substantially weaker. However, a 3,4-dimethyl substituted analog with an O-substituted pyrimidine, compound **III**, bound with increased affinity (IC_{50} = 2.9 ± 0.2 μM). Finally, when the pyrimidine oxygen was changed to a nitrogen, we observed an increase in potency with IC_{50} values of 1.3 ± 0.2 μM and 1.7 ± 0.4 μM for the 3,4- and 3,5-dimethyl analogs, compounds **IV** and **V**, respectively, against BRD4(1). Molecule **VI**, with a 3,5-difluoro substituted aromatic ring (Scheme 4) versus methyl groups did not interact with high affinity (IC_{50} > 250 μM), supporting the need for an electron rich ring. A direct binding titration of compounds **IV** and **V** by isothermal titration calorimetry (ITC) determined entropically favorable binding events leading to a K_d of 1.8 μM and 1.2 μM, respectively (Fig.S7).

Scheme 2: Synthesis of Compounds **I**, **II** and **III**

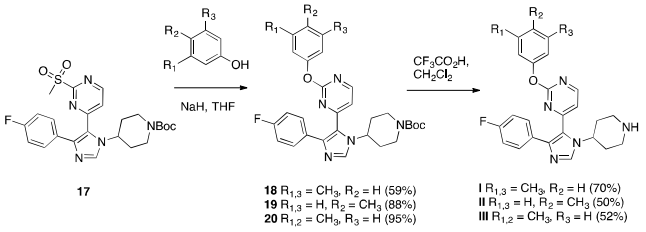

Scheme 3: Synthesis of Compounds **IV** and **V**

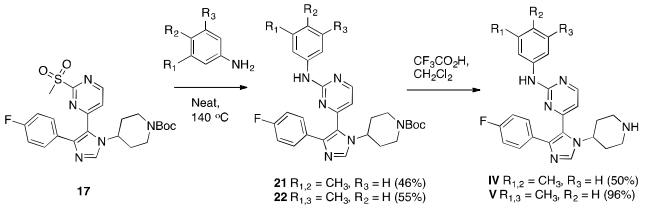

Scheme 4: Synthesis of Compound **VI**

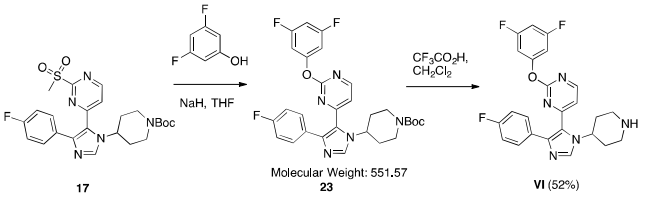

To evaluate if these molecules would function as pan-BET inhibitors based on binding to both BRDT(1) and BRD4(1), we next tested D1 vs. D2 selectivity, as our fluorescent tracer binds to D2s of BRDT and BRD4 with high affinity (K_d = 270 and 183 nM). Surprisingly, in all cases, the analogs tested were unable to fully displace BI-BODIPY from either D2 construct (Fig.2B). Alternatively, pan-BET inhibitor BI2536[28] displaced the fluorescent tracer from both domains of BRDT and BRD4. A D2-selective inhibitor RVX-208 was tested in a similar fashion to further validate the experimental outcomes seen with our constructs (Fig.S2 and S3). Additionally, a dual bromodomain construct of BRD4 was tested in our FA assay, and only partial displacement was observed with compound **V**, consistent with only fully displacing BI-BODIPY from the first bromodomain (Fig.S4). Molecules **I-III** also maintained their selectivity for D1 over D2 when tested against BRDT(2), indicating that neither the substitution pattern on the aromatic ring nor the O to N substitution on the pyrimidine ring was responsible for the observed selectivity.

The observed preference towards BRD4(1) led us to evaluate selectivity against the two other BET proteins, BRD2 and BRD3, using an orthogonal assay. Compound **V** was assayed commercially against seven of the eight BET bromodomains in an ALPHAScreen format.[29] While BRDT(2) was not available for testing by ALPHAScreen, D1 over D2-selectivity was

maintained for compound **V** (Table 1 and Fig.S8). Additionally, compound **V** displayed 6- and 16-fold selectivity for BRD4 over ubiquitously expressed BET proteins BRD2 and BRD3, respectively (Fig.S8). Together, these results support a valuable scaffold for developing D1-selective inhibitors of BET bromodomains, albeit with the highest affinity for BRD4(1) and BRDT(1).

Structural Analysis of Binding

Due to the paucity of D1-selective inhibitors and the generality of these results within the trisubstituted imidazole scaffold, we sought to structurally characterize their interactions. Protein-observed fluorine NMR (PrOF NMR) is an emerging method for ligand discovery that has been used to characterize the binding interface of small molecules with bromodomains,[30] as well as quantify the affinity of weak binding molecules via chemical shift perturbation experiments over a range of ligand concentrations.[31] PrOF NMR was used to characterize the binding interactions of compound **V** with both BRD4(1) and BRDT(1) (Fig.3A), and to further test selectivity against additional bromodomains at higher small molecule concentrations than was tolerated in earlier experiments. Our focus in these experiments was primarily on the WPF shelf tryptophan residue adjacent to the K_{ac} binding site, W81 for BRD4(1) and W50 for BRDT(1), to see if an unusual effect on resonance perturbation was observed relative to our prior reports.[26] In both BRD4(1) and BRDT(1), using compound **V**, an intermediate-to-slow exchange perturbation of the WPF shelf resonance was observed that reached the fully bound state at approximately 1 eq. of small molecule. Such NMR behavior is indicative of a residence time on the protein that is sufficiently long on the NMR time scale to partially resolve both the bound and unbound states and is consistent with binding site and affinity of the single digit micromolar K_d exhibited for these domains by compounds **IV** and **V**.[32] W44 of BRDT(1) is outside the

binding site and was also minimally perturbed, indicating a conformational change of the protein. However these data did not support binding to a new binding site, and was similar to observations in our prior reports.[26] We further tested non-BET bromodomains of BPTF, and a yeast GCN5-like malarial protein that also contains a WPF-shelf. In these cases, we did not detect binding to either protein, consistent with selectivity for the BET family of bromodomains (Fig.S9).

We turned to X-ray crystallography to obtain higher resolution structural information to understand the mode of molecular recognition and to rationalize the domain selectivity. Trisubstituted imidazoles, SB-251527 and SB-284847-BT, have previously been crystallized with BRD4(1) (PDB ID: 4O7F and 4O7B, respectively)[25]. In addition, we crystallized compounds **IV** and **V**, with BRD4(1) (Fig.3C). All four compounds engage the protein in a similar fashion with the imidazole making direct hydrogen bonding interactions with N140, which is displaced by 0.8 Å relative to the apostructure along with a displacement of the Cα of the adjacent K141 by 2.2 Å (Fig.3D, E and S11). However, unlike pan- BET inhibitors, these molecules failed to hydrogen bond to Y97 via a bridging structured water. The O-N substitution pattern did alter the orientation of the aromatic ring slightly, which may favor edge to face π-π interactions with W81 of BRD4(1) in a lipophilic region adjacent to the WPF shelf (Fig.S12) to impact affinity but not selectivity. The methyl groups were necessary for binding affinity, as a 3,5-difluoro substituted analog **VI** only bound weakly to both bromodomains of BRD4. Overlay of a BRD4(2) crystal structure shows potential steric incompatibilities at multiple regions of the small molecule, including a steric clash of the C2 imidazole portion of the ring of compounds **IV** and **V** with N433 in the binding site which may not be as conformationally flexible as the BRD4(1) N140 due to the adjacent P434. These incompatibilities may preclude a high affinity

interaction with BRD4(2); however, such a steric effect could not be directly proven from our structures. Together ^{19}F-NMR and X-ray structural analysis could be used to rationalize binding interactions but was not sufficient to describe selectivity.

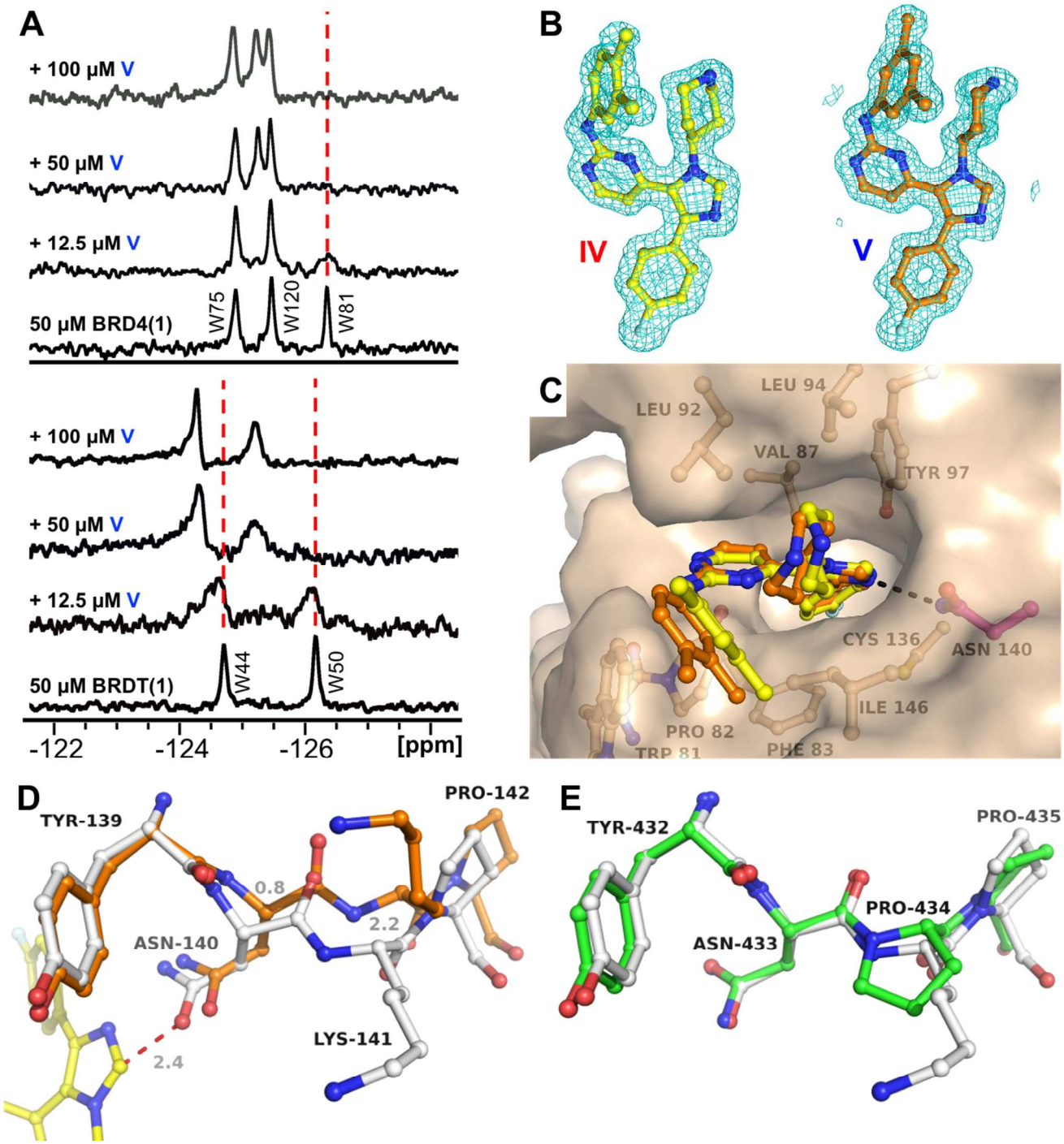

Figure 3: Confirmation of compound **V** binding BRD4(1) and BRDT(1), and possible structural basis for D1 over D2 selectivity of inhibitors. **A**. PrOF NMR titrations with bromodomains of BRD4 and BRDT. Samples contain 50 μM ^{19}F-labelled BRD4(1) or BRDT(1) with increasing concentrations of ligand **V**. **B**. Electron density maps (2Fo-Fc; 1σ) from X-ray structures of BRD4(1) liganded with **IV** (yellow, 1.74 Å, PDB ID: 6MH7) and **V** (orange, 1.60 Å, PDB ID: 6MH1). **C**. Superposition of compounds **IV** and **V** in the K_{ac} site of BRD4(1) reveals subtle conformational changes of the dimethylphenyl moieties nested in the WPF shelf. **D**. In the unliganded state of BRD4(1) (grey, PDB ID: 4IOR), the K_{Ac} site around Asn140 is in a relaxed state. Upon binding of inhibitor (orange structure) Asn140 gives way (Δ = 0.8 Å) due to steric hindrance with the imdiazole moiety of the inhibitor (red dotted line), and positions itself for optimal H-bonding interaction. As a result, the adjacent Lys141 undergoes a large conformational change (Δ = 2.2 Å). **E**. In unliganded BRD4(2) (green, PDB ID: 2OUO), the region around Asn433 is highly similar to BRD4(1) (grey) except for the presence of Pro434 for lysine. The geometric constraints of the Asn-Pro-Pro sequence in BRD4(2) likely renders the peptide more rigid and less compatible with the inhibitor-induced conformational changes observed in BRD4(1).

As an alternative possibility for selectivity, we considered the sequence similarity between BET-D1 and D2. Of the three non-conserved amino acids between the binding sites, we hypothesized the proximity of the piperdyl group to D144 in our crystal structures was potentially responsible for the observed selectivity trends. This BET D1-conserved aspartic acid is replaced by a histidine (H437 of BRD4) in BET-D2s. At physiological pH, H437 will be weakly protonated, and may result in potential electrostatic repulsions in addition to steric effects that prevent binding to D2. To determine whether the origins of D1 vs D2 selectivity are due to

H437 in D2, we expressed a H437D mutant of BRD4(2) construct to restore binding of compound **V**. For this experiment, we used a new fluorescent tracer for a FA assay, based on a fluorescein-labeled (+)-JQ1 molecule. (+)-JQ1 bound to H437D BRD4(2) with comparable affinity to the WT D2 protein in direct binding assays (Fig.S5; K_d BRD4(2) = 120 nM, BRD4(2) H437D = 200 nM), with a slightly attenuated IC_{50} in competition assays (IC_{50} BRD4(2) = 490 nM, BRD4(2)-H437D = 590 nM). Binding of **V** to BRD4(2)-H437D however was not observed (Fig.S6), suggesting the observed selectivity trends are not entirely attributable to H437 of BRD4(2).

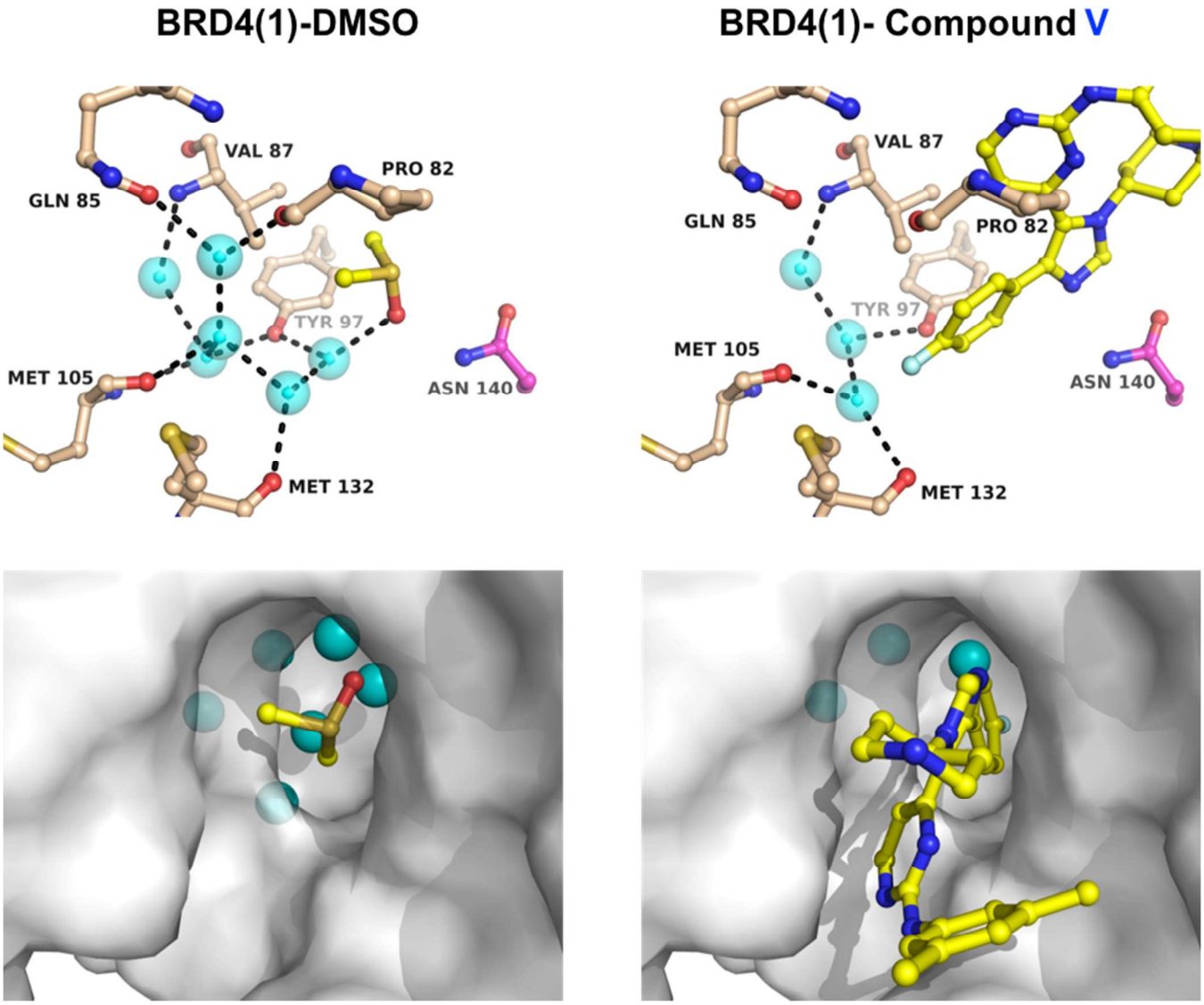

Figure 4: Displacement of Structured Waters from BRD4(1). Crystal structure of BRD4(1) with DMSO (left, yellow PDB ID: 4IOR) and Compound **V** (right, yellow PDB ID: 6MH1), where structurally conserved water molecules are shown in cyan.

Displacement of Structured Waters

Recent computational studies suggest a second possible explanation for the observed selectivity based on differential affinities for the four structured waters within the BET bromodomain binding sites. In these reports, the stability of bromodomain water networks have identified the water molecules most likely to be displaced are in BRD4(1) and BRDT(1) amongst the other BET bromodomains,[33,34] whose water molecules are more tightly bound to the protein. Such an effect would also explain the observed selectivity of compound **V** for BRD4(1) and BRDT(1) over the other BETs measured in the ALPHAScreen assay. We compared the co-crystal structure of compound **V** with BRD4(1) and a DMSO molecule bound to the same protein (Fig.4). Whereas in the DMSO co-structure six water molecules are present including the four conserved structured waters, three water molecules are displaced in the co-crystal structure with compound **V**, and the water network is reorganized by the fluorophenyl group of compound **V**. Similar displacements were observed in the co-crystal structure with compound **IV** (not shown). Displacement of water in the binding site is also consistent with the positive entropy of binding in ITC experiments with compounds **IV** and **V** (5.0 and 4.2 cal/mol/deg respectively). Importantly, this mode of binding and selectivity are not observed in BET-D1 selective molecules **4** (Olinone) and **5** (MS-436), however a remarkably similar binding mode has been observed in a selective TRIM24 bromodomain inhibitor.[35] These results may in part give rise to our observed selectivity, but the generality of such a finding will be useful to study in future investigations.

Table 1: ALPHAScreen analysis of compounds **V**, **VII**, **VIII** and **IX** against 7 of 8 BET bromodomains

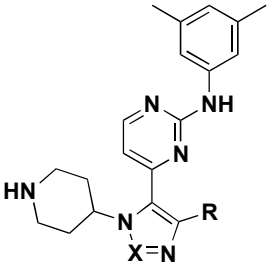	R	X	IC_{50} by ALPHAScreen (µM)						
			BRD4		BRD3		BRD2		BRDT
			D1	D2	D1	D2	D1	D2	D1
V	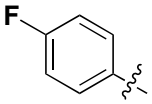	**C**	1.8	>100	11.2	>100	29	67	5.3
VII	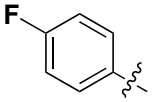	**N**	27	75	51	110	43	30	36
VIII	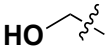	**N**	160	102	200	310	>250	260	110
IX		**N**	1.3	0.56	0.77	2.4	1.8	12	1.6

To further evaluate the displacement of structured waters by the fluorophenyl group and additional effects around the imidazole ring which removes steric effects from a C-H at position C2, we synthesized three new molecules (**VII**, **VIII**, and **XI**), based on a 1,4,5-trisubsititued triazole scaffold (Scheme 5). These molecules either maintain the fluorophenyl group for a direct comparison with **V**, or replace this phenyl group with a smaller hydroxymethyl or methyl group

to maintain the structured waters. Compound **VII** bound BRD4(1) by PrOF NMR in a manner similar to compound **V** (Fig.S10). But due to solubility challenges at high concentrations and the low sensitivity of FA, ALPHAScreen was used to test for BET selectivity. Replacement of the imidazole ring with a triazole in compound **VII** resulted in a moderate loss of potency to BRD4(1) (IC_{50} = 1.8 μM for **V** vs. 27 μM for **VII**) likely due to the weakened hydrogen bonding with conserved N140 of BRD4 and a significant loss of selectivity (27 μM D1 vs 76 μM D2) Replacement of the fluorophenyl group with a methoxy (**VIII**) group resulted in further reduced binding with IC_{50} > 100 μM, possibly due to the hydrophobic nature of the binding pocket. Finally, in contrast, truncation of the fluorophenyl group to a methyl in compound **IX** enhanced binding 20-fold relative to **VII** (IC_{50} = 1.3 μM for **IX** vs 155 μM for **VII**). The large gain in potency indicates an energetic penalty must be overcome for displacing the structured waters with a large aromatic group. In the case of compound **IX**, which lacks a large aromatic group displacing structured waters, an inversion of BRD4 domain selectivity favoring BRD4(2) (IC_{50} = 0.56 μM), and overall pan-BET inhibition were observed.

Scheme 5: Synthesis of triazoles **VII**, **VIII** and **IX**

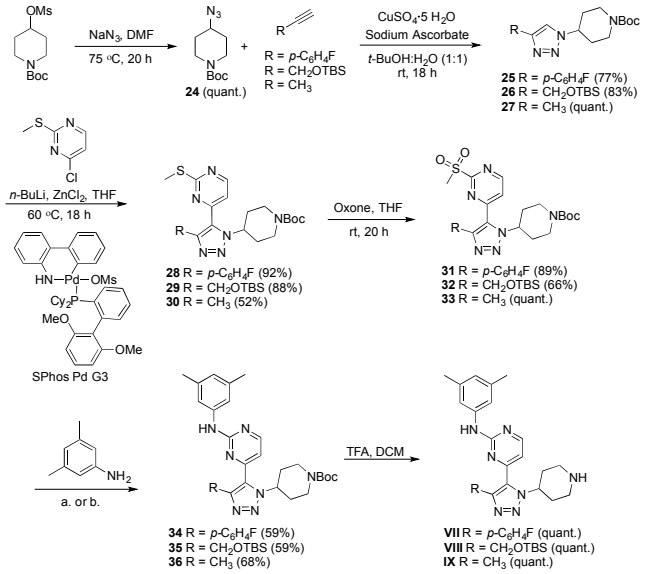

Reagents & Conditions: (a) 100 ^{o}C, 3 h for synthesis of **34** and **36**, or (b) NaHMDS, -78 ^{o}C, 0.5 h for **35**

From these data, we conclude that the D1 over D2 selectivity cannot be attributed to the methyl-substitution pattern of the pyrimidine-substituted aromatic ring, the phenoxy-pyrimidine to anilino-pyrimidine substitution, or even steric incompatibilities with the piperdyl group. Rather, the observed selectivity is due to a combination of effects including the imidazole ring itself, and from the fluorophenyl ring displacing structured waters.

Bromodomain and Kinase Selectivity Profiling

To more broadly test the bromodomain selectivity of compound **V**, we used a commercial assay platform to characterize the activity against 32 of the 61 bromodomains provided by DiscoverX. Based on a measured K_d of 1.2 μM, we tested the selectivity of **V** at 10 μM (approximately 10-fold above the K_d). Consistent with our FA and ALPHAScreen results, the two most significant interactions of the eight BET bromodomains with **V** were with BRD4(1) and BRDT(1), with 86% and 50% inhibition at that concentration, respectively (Table S3). The BET D2s were the most unaffected (7-27% inhibition) relative to D1. Overall, only bromodomains, SMARCA2, PCAF, p300, and SMARCA4 had inhibitory activity between 40-50%. These results demonstrate the selectivity of compound **V** towards BET D1s and given the modular synthesis of the 1,4,5-trisubstituted imidazole scaffold, represent a useful starting point for domain-selective inhibitor development.

As compound **I** is a reported MAP-kinase inhibitor, we were interested in verifying the selectivity of these analogs against other kinases. Similar analogs of **I** either maintaining pyrimidyl-aniline substitutions but lacking dimethyl groups, or containing methylated piperidinyl groups have been previously reported, where both compounds are highly potent and selective for p38α and β at 100 nM.[36] As such, we expected similar affinity for p38α and a similar kinase

selectivity profile. Indeed, the K_d of analog **V** against p38α was determined to be 0.47 nM (Fig.S13). Due to the weaker D1 potency, we tested for selectivity amongst kinases at a concentration of 1 μM using the DiscoverX platform. In this case, we measured high inhibitory activity against p38α and β (Table S4). However, additional kinases were inhibited at this concentration, giving a selectivity score S(1) of 0.037, similar to p38α chemical probe SB203580 (0.024 at 100 nM). Due to available crystal structure data of related compounds bound to p38α and the wealth of data available on this inhibitor class, kinase selectivity may be further improved and potentially even abolished through rational design.

Cellular Evaluation of Lead Compounds

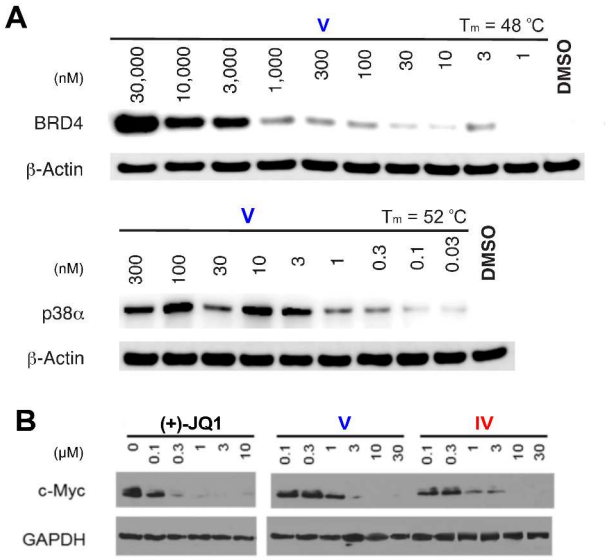

Figure 5: Cellular evaluation of lead compounds confirms target engagement. **A**. Cellular thermal shift assay with compound **V** indicates thermal stabilization of BRD4 and p38α in A549 cells, with β-actin used as a loading control. **B**. Western blots of expressed c-Myc levels in MM.1S cells, with GAPDH used as a loading control.

Given the BET D1 selectivity exhibited by compounds **IV** and **V**, we proceeded by testing these molecules in cells. First, we verified target engagement in the native chemical environment by using a CEllular Thermal Shift Assay (CETSA) in A549 cells, where thermal stability of the target protein is altered upon binding to small molecules.[37] Here, an isothermal denaturation experiment indicated compound **V** stabilized BRD4 and p38α in a dose-dependent manner at concentrations above 3 μM and 1 nM, respectively. Protein melt temperatures correlated well with previous CETSA experiments performed on BRD4 and p38α.[38,39] Importantly, as this experiment does not measure cellular outcomes downstream of target inhibition, these results confirm unambiguously that compound **V** enters cells and maintains interactions with BRD4 and p38α in a cellular context (Fig.5A).

After verifying protein target engagement, we proceeded to test the efficacy of our D1-selective inhibitors in MM.1S cells by measuring reduction of c-Myc, an oncogene highly sensitive to BET inhibition, in several leukemia cell lines. Similar to (+)-JQ1 used as a positive control, compounds **IV** and **V** inhibited expression of the c-Myc oncoprotein in MM.1S cells at concentrations approaching their respective BRD4(1) K_d values, as determined by Western blot (Fig.4B). These results also mirrored cell viability data in the cell line studied (Fig.S14). Together, these are characteristic hallmarks of BET inhibitors, and suggest effective cellular bromodomain inhibitory activity. To verify inhibition of the p38α kinase, we determined the phosphorylation states of its downstream phosphorylation target, MSK1. Here we observed a decrease in levels of MSK-1 phosphorylation at T581 upon treatment with compounds **IV** and **V**, although at levels significantly higher than their affinity for p38α. This effect was not observed with (+)-JQ1 treatment (Fig.S16). Together, these results are consistent with BET-D1 inhibition

using our 1,4,5-trisubstiuted imidazole scaffold being sufficient to regulate transcription in cells in a BRD4-specific manner.

Inhibition of Inflammation

The role BRD4 plays in coupling NF-κB signaling to gene transcription via K_{ac} recognition has been disputed. In certain systems, transcriptional activation of RelA target genes has been observed independent of BRD4,[40] whereas Chen and coworkers have reported on BRD4 maintaining activity of NF-κB signaling via recognition of K310 acetylation at the RelA subunit.[18] In the case of NF-κB dependent activity, it remains unclear whether D1 or D2 plays the dominant role in driving transcription; the two bromodomains of BRD4 maintain interactions with chromatin and the presence of both domains enhances transcription.[7] In contrast, while Zou and co-workers showed a 10-fold stronger interaction of RelA with D2 by a fluorescence-competition assay,[18] Jung et al. did not detect any binding interactions in a TR-FRET assay,[41] leading to uncertainty of a direct interaction between RelA and BRD4. Together, these data highlight a need for confirmation of the relevant interactions of each bromodomain of BRD4.

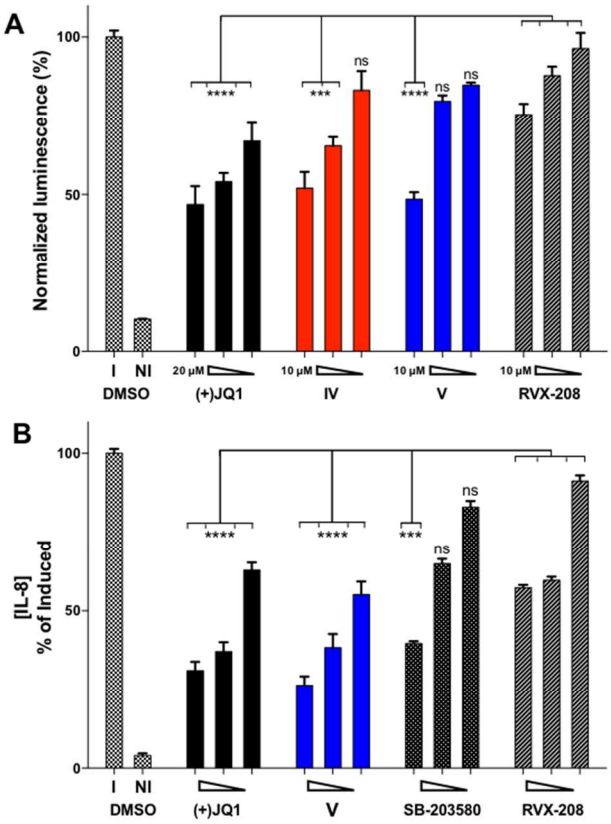

Figure 6: Inhibition of NF-κB signaling and a NF-κB target gene. **A**. NF-κB-luciferase reporter assay with A549 cells. (+)-JQ1 = 20, 5, 1 μM; **IV**, **V** and RVX-208 = 10, 5, 1 μM. **B**. Sandwich IL-8 ELISA (+)-JQ1, **V**, SB-203580 and RVX-208 = 10, 1, 0.1 μM. Data reported as Mean ± SEM values (n = 3 biological replicates) normalized to no compound-induced (I) control values. All samples except NI control were induced with 10 ng/mL TNFα. See figure S3 for compound mediated cellular cytotoxicity data. (ANOVA comparison to the three RVX-208 treatments, ns = not statistically significant; *** = $p < 0.001$ and **** = $p < 0.0001$)

To further assess cellular efficacy of our D1-selective inhibitors, we employed a luminescence-based NF-κB reporter assay in A549-NF-κB-luc cells. Compound **V** (51% inhibition at 10 μM) produced the most effective knockdown of TNFα-induced transcription in this assay, compared

to inhibition of BRD4(2) using RVX-208 (25% inhibition at 10 μM) (Fig.6A). As other p38 MAPK inhibitors SB-203580 and VX-702 showed limited inhibitory effects in this assay (Fig.S17), and compounds **IV** and **V** exhibited minimal cytotoxicity towards A549 cells up to concentrations of 25 μM and 10 μM, respectively (Fig.S14), these experiments suggest BRD4(1) inhibition may be crucial to NF-κB signaling in A549 cells and support earlier results using BET selective inhibitor MS-611.[21]

Inhibition of BET bromodomains has been shown to decrease production of cytokines; however, the role of individual BET bromodomains here is also yet to be deconvoluted. To assess the effect of compound **V** on inflammation at the protein level, we quantitated the suppression of cytokine production using an immunosorbent assay (ELISA). We chose to measure the concentrations of secreted cytokine IL-8, since its role as an inflammatory stimulus for neutrophil recruitment has been well characterized.[42] At concentrations of 1 μM in this assay, BRD4(1) inhibition using compound **V** reduced levels of cytokine production (62% inhibition at 1 μM) more effectively than BRD4(2) inhibition by RVX-208 (40% inhibition at 1 μM). Moreover, the effects of compound **V** were comparable to pan-BET inhibition by (+)-JQ1 (63% inhibition at 1 μM) (Fig.6B). This increased potency of **V** is likely due to the additional inhibition of p38α. However, other off-targets cannot be ruled out at this point. Interestingly, complete inhibition of cytokine production was not observed with any of these molecules, whereas an irreversible NF-κB inhibitor, parthenolide, decreased IL-8 production to baseline at 20 μM.[43] These results, coupled with confirmation of target occupancy by CETSA, establish a potential mode of synergy via dual targeting of p38α and BET bromodomains.

Discussion

Through a late stage structure-activity relationship (SAR) investigation of 1,4,5-trisubstituted imidazoles, we identified a small series of BET inhibitors. Biophysical characterization of lead compounds against the entire BET family revealed an unexpected but high selectivity towards BET D1s over D2s, with highest affinity for BRD4(1). Our experimental data ruled out selectivity towards N-terminal BET bromodomains due to steric hindrance by a histidine present in C-terminal BET bromodomains, where the corresponding position is occupied by aspartic acid in BET D1s (D144 in the case of BRD4). Although H437 appears within 3Å of the piperidyl group in overlays of BRD4(2) crystal structures (eg. PDB ID: 2YEM), this amino acid adopts alternate conformations that may accommodate the ligand (eg. PDB ID: 5UEU).

Rather, our data with compounds **VII** to **IX** indicate selectivity was largely due to the fluorophenyl moiety and the imidazole ring itself. Structural analysis indicates a similar binding mode of suitably substituted imidazole rings to that of acetyl groups on acetylated histones, with hydrogen bonding to a conserved asparagine residue (N140 in the case of BRD4(1)) by the imidazole ring nitrogen, although N140 and K141 are slightly displaced to accommodate the imidazole ring. Additionally, the fluorophenyl group sits much deeper in the binding pocket than previously reported BET inhibitors and is able to displace three water molecules present in the co-crystal structure of BRD4(1) with DMSO, in which one of these is a structurally conserved water. Our data and previous computational studies on the stability of bromodomain water networks[33,34] lead us to believe our observed selectivity profile also arises in part from the displacement of a conserved water from BRD4(1) and BRDT(1), but not other BET bromodomains.

Cellular data indicates our compounds are highly cell permeable and capable of engaging BRD4 in various cell lines. However, whereas effects on the MM.1S cell line appear to be

largely BRD4-driven due to the Myc sensitivity of this cell line, the A549 lung cancer cell line appears to be increasingly sensitive to both p38α and BRD4 inhibition, based on decreases in cytokine secretion upon treatment with our molecules. While such cooperative effects can only be cautiously assigned due to additional off-target kinase engagement, our preliminary evaluations suggest selective inhibition of BRD4(1) may be more efficacious than BRD4(2) inhibition. These cellular data confirm previous chromatin binding studies and work targeting inhibition of BET bromodomains in inflammation,[44,45] however bromodomain inhibition alone failed to completely inhibit signaling pathways in the system studied here.

Although kinase activity was secondary to our aim of developing selective BET inhibitors, we endeavored to fully characterize the kinase activity of our lead molecules. Previous reports on substituted imidazoles and pyrazoles of the 'DFG-out' class of hinge-binding kinase inhibitors suggest modest additions to the periphery of the scaffold, such as through N-alkylation, may improve selectivity.[46,47] Additionally, by replacing the *p*-fluorophenyl moiety from similar trisubstituted imidazoles with ethyl- or chloro- groups, Gallagher et al. observed a loss of p38α kinase inhibition.[48] We thus envision the selectivity profile of these molecules may be readily improved by further analog synthesis and SAR studies.

Conclusion

Through a systematic investigation of a recently characterized 1,4,5-substituted imidazole scaffold, and newly reported 1,4,5-substituted triazole scaffold, we have described a new BET inhibitor class with high selectivity for D1 over D2 for BRD4 and BRDT. From a therapeutic standpoint, this class of 1,4,5-trisubstituted imidazoles and triazoles may be a valuable starting point for dual kinase/bromodomain inhibition, as simultaneous BRD4 and MAP/PI3 kinase inhibition has recently been suggested for synergistic treatment of colon cancer, avoiding the

development of resistance to BET or kinase inhibitor monotherapy,[28,49] and resulting in decreased toxicity relative to a cocktail of (+)-JQ1 and PI3K inhibitors.[50] As demonstrated here, the optimization of further inhibitors of individual BET D1s may enable selective control of BRD4-associated inflammatory signaling. Finally, the displacement of structured waters may also be a general strategy that can be applied to other known pan-BET inhibitors which we are actively investigating.

Experimental Section

General Synthetic Methods: All chemical reagents were purchased from commercial vendors and used without further purification. Flash chromatography of compounds was performed on a Teledyne-Isco Rf-plus CombiFlash instrument across RediSep Rf columns. ^{1}H (400 MHz) and ^{13}C (125 MHz) NMR spectra were recorded in Chloroform-*d* or Methanol-d_4 and chemical shifts (δ) are reported in ppm. All coupling constants (J) are reported in hertz (Hz), where s = singlet, d = doublet, t = triplet, and m = multiplet. Purity of final compounds diluted in DMSO was determined by reverse-phase high performance liquid chromatography (HPLC) analysis using an Agilent 1200 Series HPLC (detector: 215 and 245 nm DAD; column: Agilent Zorbax SBC18, 4.6 × 150 mm, 5.0 µm; mobile phase gradient: 90:10 to 15:85 0.1% TFA in H_2O: Acetonitrile over 22 minutes; flow rate, 1.0 mL/min), where all compounds used were verified to be >95% purity by peak area. High-resolution mass spectrometry was performed using positive mode electrospray ionization methods (ESMS) with a Bruker BioTOF II spectrometer.

Synthesis of Common Intermediate 12:

Synthesis of 4-methylbenzenesulfinic acid (7): To a suspended solution of *p*-toluenesulfinic acid sodium salt **6** (3.0 g, 16 mmol) in water (10.0 mL) was added methyl tert-butylether (5.0 mL) followed by drop-wise addition of conc. HCl (1.5 mL). After stirring the reaction for 5 min.,

the organic phase was separated, and the aqueous phase was extracted with methyl tert-butylether (2 x 25 mL). The combined organic phase was dried over anhydrous magnesium sulfate and concentrated under reduced pressure. The solid obtained was re-suspended in hexanes (50 mL) and was filtered and dried to give the desired compound 2 as a white solid (2.4 g, 91%).

Synthesis of N-((4-fluorophenyl)(tosyl)methyl)formamide (8): A mixture of 4-methylbenzenesulfinic acid **7** (0.50 g, 3.2 mmol), 4-fluorobenzaldehyde (0.58 g, 4.7 mmol), formamide (0.52 g, 12 mmol) and camphorsulfonic acid (0.09 g, 0.4 mmol) was stirred at 60 °C for 18 h. The resulting solid was stirred with a mixture of methanol (0.8 mL) and hexanes (1.9 mL). The solid was filtered and was re-suspended in methanol/hexanes (1:3, 4.5 mL) and was stirred to obtain a fine suspension. The suspension was filtered and dried to give the pure compound **8** as a white solid (0.64 g, 65%). ^{1}H NMR (500 MHz, $CDCl_3$) δ: 8.06 (s, 1H), 7.69 (d, 2H, J = 8.3 Hz), 7.43-7.4 (m, 2H), 7.31 (d, 2H, J = 7.8 Hz), 7.06 (t, 2H, J = 8.3 Hz), 6.29 (s, 1H), 2.43 (s, 3H).

Synthesis of 1-fluoro-4-(isocyano(tosyl)methyl)benzene (9): To a solution of *N*-((4-fluorophenyl)(tosyl)methyl)formamide **8** (0.20 g, 0.65 mmol) in 1,2-dimethoxyethane (3.5 mL) at -10 °C was added $POCl_3$ (0.15 mL, 1.6 mmol) followed by Et_3N (0.46 mL, 3.3 mmol) keeping the internal temperature below -5 °C. The reaction was warmed to room temperature and was stirred for 2 h. The reaction mixture was quenched by addition of ice-cold water and the aqueous phase was extracted with methyl tert-butylether (2 x 15 mL). The combined organic phase was washed with saturated aqueous $NaHCO_3$ (1 x 10 mL), brine (1 x 10 mL) and was concentrated under reduced pressure. The residue was triturated with hexanes to give the desired product as a

brown solid (0.11 g, 55%). ^{1}H NMR (500 MHz, $CDCl_3$) δ: 7.65 (d, 2H, *J* = 8.0 Hz), 7.38-7.37 (m, 4H), 7.12 (t, 2H, *J* = 8.3 Hz), 5.61 (s, 1H), 2.5 (s, 3H).

Synthesis of 4-(dimethoxymethyl)-2-(methylthio)pyrimidine (13): A mixture of pyruvic aldehyde dimethylacetal **10** (6.0 mL, 50 mmol) and *N,N*-dimethylformamide dimethylacetal (6.0 mL, 45 mmol) was heated at 100 °C for 18 h. After cooling the mixture to room temperature, methanol (30.0 mL), thiourea (6.96 g, 91.4 mmol) and sodium methoxide (25% in MeOH, 23.1 mL, 106 mmol) were added. The reaction mixture was then stirred at 70 °C for 2 h. The reaction mixture was then cooled, iodomethane (14.4 mL, 231 mmol) was added drop-wise, and the reaction was stirred at room temperature for 3 h. The reaction mixture was then diluted with ethyl acetate (200 mL) and water (100 mL). The organic phase was separated, and the aqueous phase was extracted with ethyl acetate (2 x 100 mL). The combined organic phase was dried over anhydrous magnesium sulfate and concentrated under reduced pressure to give the corresponding product **13** as a brown oil (7.5 g, 75%). ^{1}H NMR (400 MHz, $CDCl_3$) δ: 8.56 (d, 1H, *J* = 5.1 Hz), 7.19 (d, 1H, *J* = 4.9 Hz), 5.19 (s, 1H), 3.42 (s, 6H), 2.58 (s, 3H).

Synthesis of 2-(methylthio)pyrimidine-4-carbaldehyde (14): A solution of 4-(dimethoxymethyl)-2-(methylthio)pyrimidine **13** (2.0 g, 10 mmol) in 3*N* HCl (8.4 mL, 25 mmol) was stirred at 48 °C for 16 h. The reaction was cooled and quenched by addition of solid Na_2CO_3. The residue was washed with ethyl acetate (3 x 50 mL). The combined organic phase was dried and concentrated to give the crude product which was purified by filtration over a pad of silica gel eluting with dichloromethane to give the pure product as a pale yellow solid (0.6 g, 40%). ^{1}H NMR (400 MHz, $CDCl_3$) δ: 9.96 (d, 1H, 0.6 Hz), 8.77 (dd, 1H, *J* = 4.8, 0.5 Hz), 7.45 (d, 1H, *J* = 4.8 Hz), 2.64 (s, 3H).

Synthesis of tert-butyl 4-(((2-(methylthio)pyrimidin-4-yl)methylene)amino)piperidine-1-carboxylate (15): To a solution of 2-(methylthio)pyrimidine-4-carbaldehyde **9** (0.20 g, 1.3 mmol) and *tert*-butyl 4-aminopiperidine-1-carboxylate (0.26 g, 1.3 mmol) in dichloromethane (3 mL) was added anhydrous magnesium sulfate (0.31 g, 2.6 mmol) and the reaction was stirred at room temperature for 24 h. After confirmation of the completion of reaction by TLC, the reaction mixture was filtered, and the solvent was evaporated to give the desired product which was taken directly to the next step.

Synthesis of tert-butyl 4-(4-(4-fluorophenyl)-5-(2-(methylthio)pyrimidin-4-yl)-1H-imidazol-1-yl)piperidine-1-carboxylate (16): A mixture of *tert*-butyl 4-(((2-(methylthio)pyrimidin-4-yl)methylene)amino)piperidine-1-carboxylate **15** (0.44 g, 1.3 mmol), 1-fluoro-4-(isocyano(tosyl)methyl)benzene 4 (0.38 g, 1.3 mmol) and potassium carbonate (0.18 g, 1.3 mmol) in DMF at room temperature was stirred for 48 h. The reaction mixture was quenched by the addition of water and was extracted with ethyl acetate (3 x 25 mL). The combined organic phase was washed with 5% aqueous LiCl and concentrated under reduced pressure to give the crude product which was purified by column chromatography over silica gel (60-120 mesh) using ethyl acetate and hexanes as eluent (0-60%) to give the desired product as a yellow solid (0.17 g, 28%). ^{1}H NMR (400 MHz, $CDCl_3$) δ: 8.35 (d, 1H, J = 5.2 Hz), 7.76 (s, 1H), 7.45-7.41 (m, 2H), 7.03 (t, 2H, J = 8.6 Hz), 6.79 (d, 1H, J = 5.2 Hz), 4.85 (tt, 1H, J = 12.0, 3.6 Hz), 4.31 (br s, 2H), 2.84-2.78 (m, 2H), 2.6 (s, 3H), 2.19-2.16 (m, 2H), 1.86 (dq, 2H, J = 12.3, 4.1 Hz), 1.49 (s, 9H).

Synthesis of tert-butyl 4-(4-(4-fluorophenyl)-5-(2-(methylsulfonyl)pyrimidin-4-yl)-1H-imidazol-1-yl)piperidine-1-carboxylate (17): A solution of OXONE (160 mg, 0.25 mmol) in water (1.4 mL) was added drop-wise to a solution of *tert*-butyl 4-(4-(4-fluorophenyl)-5-(2-

(methylthio)pyrimidin-4-yl)-1*H*-imidazol-1-yl)piperidine-1-carboxylate **16** (50 mg, 0.11 mmol) in THF (2.0 mL) at -10 °C. The reaction mixture was then stirred at room temperature for 24 h. The reaction mixture was quenched by addition of ice-cold water and extracted with dichloromethane (3 x 20 mL). The combined organic phase was washed with brine and concentrated under reduced pressure to give the desired product as a pale-yellow foam (45 mg, 84 %). ^{1}H NMR (400 MHz, $CDCl_3$) δ 8.50 (d, *J* = 5.4 Hz, 1H), 7.78 (s, 1H), 7.42 – 7.35 (m, 2H), 7.22 (d, *J* = 5.4 Hz, 1H), 7.03 (t, *J* = 8.6 Hz, 2H), 5.00 (tt, *J* = 12.0, 3.6 Hz, 1H), 3.72 – 3.64 (m, 4H), 3.32 (s, 3H), 2.28 – 2.11 (m, 2H), 2.00 – 1.81 (m, 2H).

Synthesis of tert-butyl 4-(5-(2-(3,5-dimethylphenoxy)pyrimidin-4-yl)-4-(4-fluorophenyl)-1H-imidazol-1-yl)piperidine-1-carboxylate (18): To a suspension of NaH (60% in mineral oil, 9 mg, 0.04 mmol) in anhydrous THF (2 mL) was added 3,5-dimethylphenol (50 mg, 0.40 mmol) in anhydrous THF (0.5 mL) drop-wise at room temperature. The mixture was stirred for 10 min. followed by the addition of *tert*-butyl 4-(4-(4-fluorophenyl)-5-(2-(methylsulfonyl)pyrimidin-4-yl)-1*H*-imidazol-1-yl)piperidine-1-carboxylate, **17** (45 mg, 0.091 mmol) in anhydrous THF (0.5 mL). The reaction mixture was stirred for 0.5 h, quenched by the addition of water and extracted with ethyl acetate (3 x 10 mL). The combined organic phase was dried and concentrated to give the product which was taken to the next step without further purification (29 mg, 59 %). ^{1}H NMR (400 MHz, $CDCl_3$) δ 8.37 (d, *J* = 5.2 Hz, 1H), 7.71 (s, 1H), 7.48 -- 7.41 (m, 2H), 7.05 (t, *J* = 8.7 Hz, 2H), 6.91 (dt, *J* = 1.5, 0.8 Hz, 1H), 6.87 - 6.79 (m, 3H), 4.69 (tt, *J* = 12.0, 3.7 Hz, 1H), 4.22 - 4.01 (m, 2H), 2.48 (d, *J* = 13.0 Hz, 2H), 2.34 (s, 6H), 1.95 - 1.88 (m, 2H), 1.70 (dd, *J* = 11.7, 4.2 Hz, 2H), 1.48 (s, 9H). ESI-MS: calc.: 543.3, found: 544.3 (M+H).

Synthesis of 2-(3,5-dimethylphenoxy)-4-(4-(4-fluorophenyl)-1-(piperidin-4-yl)-1H-imidazol-5-yl)pyrimidine (I): To a solution of compound **18** (29 mg, 0.053 mmol) in

dichloromethane (1 mL) was added trifluoroacetic acid (0.1 mL) and the reaction mixture was stirred at room temperature for 15 min. The solvent was evaporated, and the crude sample was triturated with diethylether to give the desired product **I** as a white solid (2TFA Salt; 25 mg, 70 %). ^{1}H NMR (400 MHz, CD_3OD) δ: ^{1}H NMR (400 MHz, Methanol-d_4) δ 8.41 (d, J = 5.2 Hz, 1H), 8.37 (s, 1H), 7.40 – 7.33 (m, 2H), 7.10 (t, J = 8.8 Hz, 2H), 6.87 (s, 1H), 6.85 (d, J = 5.2 Hz, 1H), 6.83 (s, 2H), 4.64 (ddd, J = 11.9, 7.9, 3.9 Hz, 1H), 3.29 – 3.25 (m, 2H), 2.61 (td, J = 13.1, 3.0 Hz, 2H), 2.26 (s, 6H), 2.15 – 2.08 (m, 2H), 1.99 (qd, J = 13.1, 4.1 Hz, 2H). ^{13}C NMR (125 MHz, Methanol-d_4) δ 165.1, 164.5 (d, J = 248.7 Hz), 162.5, 160.9 (d, J = 36.4 Hz), 160.6, 157.6, 152.9, 139.7, 139.0, 136.2, 130.9 (d, J = 8.9 Hz), 127.0, 126.4, 125.0, 119.0, 116.7, 115.9 (d, J = 22.7 Hz), 115.7, 115.4, 52.4, 43.1, 29.5, 19.9. HRMS: calc.: 444.2200, found: 444.2207. HPLC Purity: 97.2%.

Synthesis of tert-butyl 4-(4-(4-fluorophenyl)-5-(2-(p-tolyloxy)pyrimidin-4-yl)-1H-imidazol-1-yl)piperidine-1-carboxylate (19): To a suspension of NaH (60% in mineral oil, 13 mg, 0.56 mmol) in anhydrous THF (2 mL) was added *p*-cresol (66 mg, 0.62 mmol) in anhydrous THF (0.5 mL) drop-wise at room temperature. The mixture was stirred for 10 min. followed by the addition of *tert*-butyl 4-(4-(4-fluorophenyl)-5-(2-(methylsulfonyl)pyrimidin-4-yl)-1*H*-imidazol-1-yl)piperidine-1-carboxylate, **17** (70 mg, 0.14 mmol) in anhydrous THF (0.5 mL). The reaction mixture was stirred for 0.5 h, quenched by the addition of water and extracted with ethyl acetate (3 x 10 mL). The combined organic phase was dried and concentrated to give the product which was taken to the next step without further purification (65 mg, 88%). ^{1}H NMR (400 MHz, $CDCl_3$) δ 8.38 (d, J = 5.2 Hz, 1H), 7.70 (s, 1H), 7.47 – 7.39 (m, 2H), 7.26 – 7.21 (m, 2H), 7.13 (d, J = 8.5 Hz, 2H), 7.08 – 7.00 (m, 2H), 6.84 (d, J = 5.2 Hz, 1H), 4.66 (tt, J = 11.9, 3.8 Hz, 1H),

4.21 – 3.99 (m, 2H), 2.46 (t, *J* = 12.8 Hz, 2H), 2.38 (s, 3H), 1.91 – 1.84 (m, 2H), 1.70 (dt, *J* = 12.3, 6.1 Hz, 2H), 1.48 (s, 9H).

Synthesis of 4-(4-(4-fluorophenyl)-1-(piperidin-4-yl)-1H-imidazol-5-yl)-2-(p-tolyloxy)pyrimidine (II): To a solution of compound **19** (65 mg, 0.12 mmol) in dichloromethane (1 mL) was added trifluoroacetic acid (0.1 mL) and the reaction mixture was stirred at room temperature for 15 min. The solvent was evaporated, and the crude was triturated with diethyl ether to give the desired product **II** as a white solid (2TFA Salt; 35 mg, 50 %). ^{1}H NMR (500 MHz, Methanol-d_4) δ 8.55 (d, *J* = 5.1 Hz, 1H), 7.50 – 7.46 (m, 2H), 7.32 (d, *J* = 8.2 Hz, 2H), 7.25 – 7.19 (m, 4H), 6.98 (d, *J* = 5.1 Hz, 1H), 4.77 (tt, *J* = 11.6, 4.1 Hz, 1H), 3.44 – 3.36 (m, 2H), 2.76 (td, *J* = 13.0, 3.2 Hz, 2H), 2.42 (s, 3H), 2.23 – 2.09 (m, 4H). ^{13}C NMR (125 MHz, Methanol-d_4) δ 165.3, 164.6, (d, *J* = 249.3 Hz), 162.6, 161.2, 161.0, (d, *J* = 35.5 Hz), 157.7, 150.7, 138.2, 136.1, 135.4, 131.0 (d, *J* = 9.0 Hz), 130.9, 130.0, 125.8, 125.0, 121.3, 116.8, 115.9 (d, *J* = 21.8 Hz), 115.8, 52.5, 43.0, 29.4, 19.5. HRMS: calc.: 430.2043, found: 430.2041. HPLC Purity: 99.5%.

Synthesis of tert-butyl 4-(5-(2-(3,4-dimethylphenoxy)pyrimidin-4-yl)-4-(4-fluorophenyl)-1H-imidazol-1-yl)piperidine-1-carboxylate (20): To a suspension of NaH (60% in mineral oil, 9.0 mg, 0.36 mmol) in anhydrous THF (2 mL) was added 3,4-dimethylphenol (50 mg, 0.40 mmol) in anhydrous THF (0.5 mL) drop-wise at room temperature. The mixture was stirred for 10 min. followed by the addition of *tert*-butyl 4-(4-(4-fluorophenyl)-5-(2-(methylsulfonyl)pyrimidin-4-yl)-1*H*-imidazol-1-yl)piperidine-1-carboxylate, **17** (45 mg, 0.091 mmol) in anhydrous THF (0.5 mL). The reaction mixture was stirred for 0.5 h, quenched by the addition of water and extracted with ethyl acetate (3 x 10 mL). The combined organic phase was

dried and concentrated to give the product, which was taken to the next step without further purification (47 mg, 95 %). ESI-MS: calc.: 543.3, found: 544.3 (M+H).

Synthesis of 2-(3,4-dimethylphenoxy)-4-(4-(4-fluorophenyl)-1-(piperidin-4-yl)-1H-imidazol-5-yl)pyrimidine (III): To a solution of compound **20** (47 mg, 0.86 mmol) in dichloromethane (1 mL) was added trifluoroacetic acid (0.1 mL) and the reaction mixture was stirred at room temperature for 15 min. The solvent was evaporated, and the crude was triturated with diethylether to give the desired product **III** as a white solid (2TFA Salt; 30 mg, 52 %). ^{1}H NMR (400 MHz, Methanol-d_4) δ 8.53 (d, J = 5.1 Hz, 1H), 8.51 (s, 1H), 7.51 – 7.45 (m, 2H), 7.26 (d, J = 8.2 Hz, 1H), 7.24 – 7.19 (m, 2H), 7.12 (d, J = 2.5 Hz, 1H), 7.04 (dd, J = 8.1, 2.5 Hz, 1H), 6.96 (d, J = 5.1 Hz, 1H), 4.78 (dq, J = 11.9, 4.0 Hz, 1H), 3.42 – 3.33 (m, 2H), 2.73 (td, J = 13.0, 3.1 Hz, 2H), 2.33 (s, 6H), 2.25 – 2.16 (m, 2H), 2.10 (qd, J = 12.9, 3.9 Hz, 2H). ^{13}C NMR (125 MHz, Methanol-d_4) δ 165.3, 164.6 (d, J = 248.9 Hz), 162.6, 160.8, (d, J = 35.1 Hz) 157.1, 150.8, 138.3, 137.9, 136.0, 134.0, 131.1, 131.0 (d, J = 8.6 Hz), 130.3, 129.8, 125.5, 125.1, 122.3, 118.6, 116.8, 115.9 (d, J = 22.1 Hz), 115.8, 52.6, 43.0, 29.4, 18.5, 17.8. HRMS: calc.: 444.2200, found: 444.2226. HPLC Purity: 99.7%.

Synthesis of tert-butyl 4-(5-(2-((3,4-dimethylphenyl)amino)pyrimidin-4-yl)-4-(4-fluorophenyl)-1H-imidazol-1-yl)piperidine-1-carboxylate (21): A mixture of 3,4-dimethylaniline (150 mg, 1.25 mmol) and *tert*-butyl 4-(4-(4-fluorophenyl)-5-(2-(methylsulfonyl)pyrimidin-4-yl)-1*H*-imidazol-1-yl)piperidine-1-carboxylate **17** (65 mg, 0.13 mmol) in 1,4-dioxane (1 mL) were heated in a sealed tube at 140 °C for 16 h. The reaction mixture was quenched by the addition of water and extracted with ethyl acetate (3 x 5 mL). The combined organic phase was dried and concentrated to give the product which was purified by

column chromatography over silica gel (60-120 mesh) using ethyl acetate and hexanes as eluent (70-100%) (32 mg, 46 %). The product was taken to the next step without further purification.

Synthesis of N-(3,4-dimethylphenyl)-4-(4-(4-fluorophenyl)-1-(piperidin-4-yl)-1H-imidazol-5-yl)pyrimidin-2-amine (IV): To a solution of compound **21** (32 mg, 0.059 mmol) in dichloromethane (1 mL) was added trifluoroacetic acid (0.1 mL) and the reaction mixture was stirred at room temperature for 15 min. The solvent was evaporated, and the crude was triturated with diethylether to give the desired product **IV** as a pale yellow solid (3TFA Salt; 23 mg, 50 %). ^{1}H NMR (500 MHz, Methanol-d_4) δ 8.28 (d, J = 5.0 Hz, 1H), 8.23 (s, 0.5H), 7.55 – 7.46 (m, 2H), 7.35 (dq, J = 4.7, 2.4 Hz, 2H), 7.22 – 7.09 (m, 3H), 6.52 (d, J = 5.1 Hz, 1H), 5.00 (ddt, J = 12.1, 8.3, 3.8 Hz, 1H), 3.42 – 3.34 (m, 2H), 2.76 – 2.67 (m, 2H), 2.39 (dt, J = 13.3, 2.7 Hz, 2H), 2.28 (d, J = 3.6 Hz, 6H), 2.15 (qd, J = 13.2, 4.2 Hz, 2H). ^{13}C NMR (125 MHz, Methanol-d_4) δ 163.9, 161.9, 161.7, 161.4, 160.8, 158.5, 157.0, 139.9, 137.0, 136.6, 135.8, 131.6, 130.5, 130.4, 129.4, 125.4, 122.8, 119.0, 117.9, 115.4, 115.2, 112.4, 51.6, 43.1, 29.7, 18.6, 17.8. HRMS: calc.: 443.2359, found: 443.2345. HPLC Purity: 97.5%.

Synthesis of tert-butyl 4-(5-(2-((3,5-dimethylphenyl)amino)pyrimidin-4-yl)-4-(4-fluorophenyl)-1H-imidazol-1-yl)piperidine-1-carboxylate (22): A mixture of 3,5-dimethylaniline (100 mg, 0.825 mmol) and *tert*-butyl 4-(4-(4-fluorophenyl)-5-(2-(methylsulfonyl)pyrimidin-4-yl)-1*H*-imidazol-1-yl)piperidine-1-carboxylate, **17** (45 mg, 0.091 mmol) were heated in a sealed tube at 140 °C for 16 h. The reaction mixture was quenched by the addition of water and extracted with ethyl acetate (3 x 5 mL). The combined organic phase was dried over anhydrous magnesium sulfate, filtered, and concentrated under reduced pressure to give the product which was purified by column chromatography over silica gel (60-120 mesh) using ethyl acetate and hexanes as eluent (70-100%) (27 mg, 55 %). ^{1}H NMR (400 MHz, $CDCl_3$)

δ 8.25 (d, *J* = 5.1 Hz, 1H), 7.73 (s, 1H), 7.53 – 7.45 (m, 2H), 7.22 – 7.18 (m, 3H), 7.06 – 6.98 (m, 2H), 6.75 (s, 1H), 6.56 (d, *J* = 5.1 Hz, 1H), 4.86 – 4.74 (m, 1H), 4.12 (q, *J* = 7.1 Hz, 2H), 2.44 (dd, *J* = 15.7, 9.9 Hz, 2H), 2.32 (s, 6H), 1.84 – 1.69 (m, 4H), 1.46 (s, 9H).

Synthesis of N-(3,5-dimethylphenyl)-4-(4-(4-fluorophenyl)-1-(piperidin-4-yl)-1H-imidazol-5-yl)pyrimidin-2-amine (V): To a solution of compound **22** (30 mg, 0.05 mmol) in dichloromethane (1 mL) was added trifluoroacetic acid (0.1 mL) and the reaction mixture was stirred at room temperature for 15 min. The solvent was evaporated, and the crude was triturated with diethylether to give the desired product **V** as a pale yellow solid (3TFA Salt; 37 mg, 96 %). ^{1}H NMR (500 MHz, $CDCl_3$) δ 8.29 (d, *J* = 5.1 Hz, 1H), 7.80 (s, 1H), 7.51 (dd, *J* = 8.4, 5.4 Hz, 2H), 7.24 (s, 2H), 7.19 (s, 1H), 7.04 (t, *J* = 8.6 Hz, 2H), 6.76 (s, 1H), 6.58 (d, *J* = 5.1 Hz, 1H), 4.78 (tt, *J* = 12.0, 3.9 Hz, 1H), 3.15 – 3.08 (m, 2H), 2.49 – 2.40 (m, 2H), 2.34 (s, 6H), 2.12 – 2.05 (m, 2H), 1.84 (qd, *J* = 12.2, 3.9 Hz, 2H). ^{13}C NMR (125 MHz, Methanol-d_4) δ 164.4, (d, *J* = 247.6 Hz) 162.4, 160.7, 158.8, 156.0, 152.6, 148.2, 139.1, 138.2, 135.4, 130.7, (d, *J* = 8.4 Hz) 130.6, 124.8, 119.0, 115.8, (d, *J* = 22.1 Hz) 115.6, 112.6, 52.3, 48.1, 43.0, 29.5, 20.1. HRMS: calc.: 443.2359, found: 443.2388. HPLC Purity: 95.7%.

Synthesis of tert-butyl 4-(5-(2-(3,5-difluorophenoxy)pyrimidin-4-yl)-4-(4-fluorophenyl)-1H-imidazol-1-yl)piperidine-1-carboxylate (23): To a suspension of NaH (60% in mineral oil, 9 mg, 0.04 mmol) in anhydrous THF (2 mL) was added 3,5-dimethylphenol (50 mg, 0.40 mmol) in anhydrous THF (0.5 mL) drop-wise at room temperature. The mixture was stirred for 10 min. followed by the addition of *tert*-butyl 4-(4-(4-fluorophenyl)-5-(2-(methylsulfonyl)pyrimidin-4-yl)-1*H*-imidazol-1-yl)piperidine-1-carboxylate, **17** (45 mg, 0.091 mmol) in anhydrous THF (0.5 mL). The reaction mixture was stirred for 0.5 h, quenched by the addition of water and extracted with ethyl acetate (3 x 10 mL). The combined organic phase was dried and concentrated to give

the product which was taken to the next step without further purification (29 mg, 59 %). ^{1}H NMR (400 MHz, Methanol-d4) δ 8.46 (d, J = 4.9 Hz, 2H), 7.5 – 7.3 (m, 2H), 7.09 (t, 2H), 6.95 (dt, 3H), 6.87 (tt, J = 9.2, 2.3 Hz, 1H), 4.7 – 4.6 (m, 1H), 3.5 – 3.4 (m, 3H), 2.88 (td, J = 13.1, 3.0 Hz, 2H), 2.21 (d, J = 13.4 Hz, 2H), 2.10 (qd, J = 13.0, 4.1 Hz, 2H), 1.45 (s, 9H). 1.22 (s, 1H), 1.19 (s, 2H), 0.8 – 0.7 (m, 1H). ESI-MS: calc.: 551.6, found: 552.1 (M+H).

Synthesis of 2-(3,5-difluorophenoxy)-4-(4-(4-fluorophenyl)-1-(piperidin-4-yl)-1H-imidazol-5-yl)pyrimidine (VI): To a solution of compound **23** (45 mg, 0.82 mmol) in dichloromethane (1 mL) was added trifluoroacetic acid (0.1 mL) and the reaction mixture was stirred at room temperature for 15 min. The solvent was evaporated, and the crude was triturated with diethyl ether to give the desired product **VI** as a white solid (2TFA Salt; 31 mg, 56 %). ^{1}H NMR (400 MHz, Methanol-d_4) δ 8.46 (d, J = 4.9 Hz, 1H), 7.40 – 7.32 (m, 1H), 7.14 – 7.03 (m, 1H), 6.99 – 6.82 (m, 2H), 3.44 – 3.36 (m, 2H), 2.88 (td, J = 13.1, 3.0 Hz, 1H), 2.21 (d, J = 13.4 Hz, 1H), 2.10 (qd, J = 13.0, 4.1 Hz, 2H), 1.19 (s, 1H), 0.84 – 0.73 (m, 1H). ^{13}C NMR (125 MHz, Methanol-d_4) δ 163.3 (dd, $J_{C\text{-}F}$ = 248.8, 15.2 Hz), 161.1 (d, $J_{C\text{-}F}$ = 35.2 Hz), 160.6, 158.6, 154.7 (d, $J_{C\text{-}F}$ = 13.4 Hz), 136.5, 130.7 (d, $J_{C\text{-}F}$ = 8.5 Hz), 117.7, 115.6 (d, $J_{C\text{-}F}$ = 22.1 Hz), 105.8 (t, $J_{C\text{-}F}$ = 22.1, 21.5 Hz), 100.9 (t, $J_{C\text{-}F}$ = 26.1 Hz), 51.9, 43.2, 29.7. HRMS: calc.: 451.1680, found: 452.2210. HPLC Purity: 97.9%.

Synthesis of Triazoles VII-IX:

Synthesis of sulfones **31**, **32** and **33**:

Synthesis of tert-butyl 4-azidopiperidine-1-carboxylate (24): To a solution of tert-butyl 4-((methylsulfonyl)oxy)piperidine-1-carboxylate (1.1 g, 3.9 mmol) in DMF (10 mL), was added solid NaN_3 (0.48 g, 7.3 mmol). The reaction was sealed under air and heated to 75 °C. After 20 h, the reaction was cooled to room temperature. The reaction mixture was diluted with water and

extracted with ethyl acetate. The combined organic phases were washed with water and brine, dried over anhydrous magnesium sulfate, filtered, and concentrated under reduced pressure. This afforded the azide **24** quantitatively, which was used without further purification. Characterization data for this compound has been previously reported.[52]

General Click Procedure and Synthesis of tert-butyl 4-(4-(4-fluorophenyl)-1H-1,2,3-triazol-1-yl)piperidine-1-carboxylate (25): The crude oil of azide **24** (3.9 mmol, assuming quantitative yield from previous reaction) was dissolved in *t*-BuOH/H_2O (1:1, 10 mL). A separate vial was charged with alkyne (660 mg, 4.8 mmol), copper sulfate pentahydrate (40 mg, 0.16 mmol), and sodium ascorbate (170 mg, 0.84 mmol). The solution of azide was transferred into the vial containing alkyne by pipette and sealed under air. After 18 h at room temperature, the reaction mixture was diluted with water and extracted with ethyl acetate. The combined organic phases were washed with brine, dried over anhydrous magnesium sulfate, filtered, and concentrated under reduced pressure to afford the triazole (1.10 g, 77%) as a white solid. ^{1}H NMR (500 MHz, $CDCl_3$) δ 7.81 (apparent dd, J = 8.8, 5.3 Hz, 2H), 7.75 (s, 1H), 7.13 (apparent t, J = 8.7 Hz, 2H), 4.67 (tt, J = 11.6, 4.1 Hz, 1H), 4.30 (br, 2H), 2.97 (br, 2H), 2.28 – 2.22 (m, 2H), 2.00 (qd, J = 12.2, 4.4 Hz, 2H), 1.50 (s, 9H). ^{13}C NMR (126 MHz, $CDCl_3$) δ 162.7 (d, $J_{C\text{-}F}$ = 247.4 Hz), 154.5, 146.8, 127.4 (d, $J_{C\text{-}F}$ = 8.1 Hz), 126.8 (d, $J_{C\text{-}F}$ = 3.2 Hz), 117.1, 115.9 (d, $J_{C\text{-}F}$ = 21.6 Hz), 80.2, 58.3, 42.7 (br), 32.5, 28.4. ^{19}F NMR (376 MHz, $CDCl_3$) δ -113.5. IR (NaCl, thin film, cm^{-1}): 2974, 1689, 1496, 1424, 1244, 1166. HRMS (ESI): Calculated for $C_{18}H_{23}FN_4NaO_2^+$, $(M+Na)^+$ 369.1697, found 369.1682.

Synthesis of tert-butyl 4-(4-(((tert-butyldimethylsilyl)oxy)methyl)-1H-1,2,3-triazol-1-yl)piperidine-1-carboxylate (26): The General Click Procedure was used and the product **26** was isolated as a white solid in 83% yield. ^{1}H NMR (500 MHz, $CDCl_3$) δ 7.47 (s, 1H), 4.84 (s,

2H), 4.59 (tt, J = 11.6, 4.0 Hz, 1H), 4.26 (br, 2H), 2.93 (t, J = 13.1 Hz, 2H), 2.26 – 2.12 (m, 2H), 1.94 (apparent qd, J = 12.3, 4.4 Hz, 2H), 1.47 (s, 9H), 0.91 (s, 9H), 0.10 (s, 6H). ^{13}C NMR (126 MHz, $CDCl_3$) δ 154.7, 148.7, 119.4, 80.3, 58.2, 58.2, 42.9 (br) 32.6, 28.6, 26.1, 18.5, -5.1. IR (NaCl, thin film, cm^{-1}): 2930, 2857, 1696, 1423, 1366, 1244, 1168, 838, 778. HRMS (ESI): Calculated for $C_{19}H_{36}N_4NaO_3Si^+$, $(M+Na)^+$ 419.2449, found 419.2452.

Synthesis of tert-butyl 4-(4-methyl-1H-1,2,3-triazol-1-yl)piperidine-1-carboxylate (27): The crude oil of azide (3.6 mmol, assuming quantitative yield from previous reaction) was dissolved in *t*-BuOH/H_2O (1:1, 20 mL). A separate 3-neck round bottom flask was charged with copper sulfate pentahydrate (290 mg, 1.2 mmol), and sodium ascorbate (710 mg, 3.6 mmol). The solution of azide was transferred into this flask by pipette. The center neck of the flask was fitted with a condensing dewar which was filled with a dry ice/acetone bath. The other two necks were sealed with septa. The top of the condensing dewar was vented by needle and this vent remained open to avoid over pressurization. Propyne was bubbled into the solution of azide by needle until the propyne started to reflux in the condensing dewar. After 1 h at room temperature, the flask was placed on a 40 °C heating block to melt the ice that formed in the flask as a result of propyne condensation. After 4 hours at this temperature, the reaction was cooled to room temperature and mixture was diluted with water and brine and extracted with ethyl acetate. The combined organic phases were washed with brine, dried over anhydrous magnesium sulfate, filtered, and concentrated under reduced pressure to afford the triazole quantitatively as a pale green solid. ^{1}H NMR (500 MHz, DMSO-d_6) δ 7.96 (s, 1H), 4.64 (tt, J = 11.4, 3.7 Hz, 1H), 4.04 (d, J = 11.0 Hz, 2H), 2.94 (br, 2H), 2.21 (s, 3H), 2.02 (d, J = 12.2 Hz, 2H), 1.80 (qd, J = 12.2, 4.3 Hz, 2H), 1.42 (s, 9H). ^{13}C NMR (126 MHz, DMSO-d_6) δ 154.3, 142.9 (br), 121.3, 79.4, 57.3, 43.1 (br), 32.4,

28.5, 11.1. IR (NaCl, thin film, cm^{-1}): 2974, 1689, 1424, 1366, 1250, 1169, 1004. HRMS (ESI): Calculated for $C_{13}H_{22}N_4NaO_2^+$, $(M+Na)^+$ 289.1635, found 289.1632.

General Coupling Procedure and Synthesis of tert-butyl 4-(4-(4-fluorophenyl)-5-(2-(methylthio)pyrimidin-4-yl)-1H-1,2,3-triazol-1-yl)piperidine-1-carboxylate (28): A solution of triazole **25** (170 mg, 0.50 mmol) in THF (8 mL) was cooled in a dry ice/acetone bath. Then n-BuLi (0.26 mL, 2.5 M in Hexanes, 0.65 mmol) was added dropwise. After 10 min, a freshly prepared solution of $ZnCl_2$ (110 mg, 0.78 mmol) in THF (1 mL) was added dropwise. After 10 min, a freshly prepared solution of SPhos Pd G3 (17 mg, 22 μmol) in THF (1 mL) was added followed by addition of chloro-pyrimidine (0.12 mL, 1.0 mmol). The reaction was heated to 60 °C. After 1.5 h, the reaction mixture was diluted with water and extracted with ethyl acetate. The combined organic phases were washed with brine, dried over anhydrous magnesium sulfate, filtered, and concentrated under reduced pressure. Final purification by column chromatography (0-50% EtOAc in Hexanes) yielded the product as a white solid (210 mg, 88%).^{1}H NMR (400 MHz, $CDCl_3$) δ 8.50 (d, J = 5.1 Hz, 1H), 7.50 (apparent dd, J = 8.6, 5.4 Hz, 2H), 7.09 (apparent t, J = 8.7 Hz, 2H), 6.86 (d, J = 5.1 Hz, 1H), 4.96 (tt, J = 11.4, 4.0 Hz, 1H), 4.30 (br, 2H), 2.89 (br, 2H), 2.61 (s, 3H), 2.42 – 2.28 (m, 2H), 2.23 – 2.06 (m, 2H), 1.50 (s, 9H). ^{13}C NMR (101 MHz, $CDCl_3$) δ 173.9, 163.1 (d, J_{C-F} = 248.9 Hz), 158.0, 155.3, 154.6, 146.3, 130.3 (d, J_{C-F} = 8.3 Hz), 129.3, 126.4 (d, J_{C-F} = 3.3 Hz), 116.5, 116.0 (d, J_{C-F} = 21.8 Hz), 80.0, 57.8, 43.0 (br), 32.3, 28.4, 14.1. ^{19}F NMR (376 MHz, $CDCl_3$) δ -112.2. IR (NaCl, thin film, cm^{-1}): 2976, 2930, 2863, 1692, 1550, 1506, 1420, 1349, 1243, 1158, 997, 913, 841, 732. HRMS (ESI): Calculated for $C_{23}H_{27}FN_6NaO_2S^+$, $(M+Na)^+$ 493.1792, found 493.1774.

Synthesis of tert-butyl 4-(4-(((tert-butyldimethylsilyl)oxy)methyl)-5-(2-(methylthio)pyrimidin-4-yl)-1H-1,2,3-triazol-1-yl)piperidine-1-carboxylate (29): A solution

of triazole **26** (830 mg, 2.1 mmol) in THF (15 mL) was cooled in a dry ice/acetone bath. Then *n*-BuLi (1.1 mL, 2.5 M in Hexanes, 2.7 mmol) was added dropwise. After 10 min, a freshly prepared solution of $ZnCl_2$ (370 mg, 2.7 mmol) in THF (5 mL) was added dropwise. After 10 min, a freshly prepared solution of SPhos Pd G3 (71 mg, 91 μmol) in THF (5 mL) was added followed by addition of chloro-pyrimidine (0.36 mL, 3.1 mmol). The reaction was heated to 60 °C. After 18 h, the reaction mixture was diluted with water and extracted with ethyl acetate. The combined organic phases were washed with brine, dried over anhydrous magnesium sulfate, filtered, and concentrated under reduced pressure. Final purification by column chromatography (0-80% EtOAc in Hexanes) yielded the product as a white solid (990 mg, 92%). ^{1}H NMR (500 MHz, $CDCl_3$) δ 8.64 (d, *J* = 5.2 Hz, 1H), 7.71 (d, *J* = 5.1 Hz, 1H), 5.24 (tt, *J* = 11.3, 4.0 Hz, 1H), 4.83 (s, 2H), 4.28 (br, 2H), 2.88 (br, 2H), 2.58 (s, 3H), 2.28 (qd, *J* = 11.8, 4.1 Hz, 2H), 2.18 – 2.11 (m, 2H), 1.47 (s, 9H), 0.87 (d, *J* = 2.6 Hz, 9H), 0.09 (s, 6H). ^{13}C NMR (126 MHz, $CDCl_3$) δ 173.2, 158.4, 154.7, 154.6, 146.9, 131.6, 116.3, 80.0, 58.1, 57.1, 42.9, 32.4, 28.5, 25.9, 18.3, 14.2, -5.1. IR (NaCl, thin film, cm^{-1}): 2929, 2856, 1697, 1542, 1419, 1157, 837. HRMS (ESI): Calculated for $C_{24}H_{40}N_6NaO_3SSi^+$, $(M+Na)^+$ 543.2544, found 543.2529.

Synthesis of tert-butyl 4-(4-(((tert-butyldimethylsilyl)oxy)methyl)-5-(2-(methylthio)pyrimidin-4-yl)-1H-1,2,3-triazol-1-yl)piperidine-1-carboxylate (30): A variation of the general coupling procedure was used. After the addition of SPhos Pd G3 and the electrophile **27**, the reaction was heated to 60 °C for 3.5 h. Final purification by column chromatography (0-60% IPA in hexanes) yielded the product (210 mg, 52%) as a white solid. ^{1}H NMR (500 MHz, $CDCl_3$) δ 8.65 (d, *J* = 5.1 Hz, 1H), 7.11 (d, *J* = 5.1 Hz, 1H), 5.11 (tt, *J* = 11.3, 3.9 Hz, 1H), 4.27 (br, 2H), 2.86 (br, 2H), 2.58 (s, 3H), 2.49 (s, 3H), 2.26 (d, *J* = 10.2 Hz, 2H), 2.10 (d, *J* = 12.4 Hz, 2H), 1.47 (s, 9H). ^{13}C NMR (126 MHz, $CDCl_3$) δ 173.5, 158.1, 155.0,

154.6, 143.8, 129.6, 115.1, 79.9, 57.8, 42.6 (br), 32.2, 28.4, 14.1, 12.1. IR (NaCl, thin film, cm^{-1}): 2974, 2930, 2864, 1691, 1548, 1422, 1276, 1162, 1006. HRMS (ESI): Calculated for $C_{18}H_{26}N_6NaO_2S^+$, $(M+Na)^+$ 413.1730, found 413.1732.

General Oxidation Procedure and Synthesis of tert-butyl 4-(4-(4-fluorophenyl)-5-(2-(methylsulfonyl)pyrimidin-4-yl)-1H-1,2,3-triazol-1-yl)piperidine-1-carboxylate (31): To a solution of the thioether 28 (350 mg, 0.74 mmol) in THF (10 mL) cooled in an ice bath, a solution of Oxone (690 mg, 2.3 mmol) in water (3 mL) was added dropwise. The reaction was sealed under air and warmed to rt. After 20 h, the reaction was diluted with ice water and extracted with ethyl acetate. The combined organic phases were washed with brine, dried over anhydrous magnesium sulfate, filtered, and concentrated under reduced pressure. This afforded the sulfone **31** (330 mg, 66%) as a white solid. ^{1}H NMR (400 MHz, $CDCl_3$) δ 8.80 (d, J = 5.3 Hz, 1H), 7.50 (apparent dd, J = 8.8, 5.2 Hz, 2H), 7.41 (d, J = 5.3 Hz, 1H), 7.15 (apparent t, J = 8.6 Hz, 2H), 5.15 (tt, J = 10.6, 4.6 Hz, 1H), 4.33 (br, 2H), 3.41 (s, 3H), 2.97 (br, 2H), 2.44 – 2.16 (m, 4H), 1.48 (s, 9H). ^{13}C NMR (126 MHz, $CDCl_3$) δ 166.6, 163.4 (d, J_{C-F} = 250.2 Hz), 158.9, 157.0, 154.6, 147.7, 130.6 (d, J_{C-F} = 8.3 Hz), 128.0, 126.0 (d, J_{C-F} = 3.3 Hz), 122.8, 116.4 (d, J_{C-F} = 21.8 Hz), 79.9, 59.2, 43.3 (br), 39.1, 32.4, 28.4. ^{19}F NMR (376 MHz, $CDCl_3$) δ -110.9. IR (NaCl, thin film, cm^{-1}): 2977, 2929, 1685, 1578, 1507, 1420, 1324, 1244, 1159, 1135, 843. HRMS (ESI): Calculated for $C_{23}H_{27}FN_6NaO_4S^+$, $(M+Na)^+$ 525.1691, found 525.1688.

Synthesis of tert-butyl 4-(4-(((tert-butyldimethylsilyl)oxy)methyl)-5-(2-(methylthio)pyrimidin-4-yl)-1H-1,2,3-triazol-1-yl)piperidine-1-carboxylate (32): To a solution of the thioether **29** (290 mg, 0.56 mmol) in THF (10 mL) cooled in an ice bath, a solution of Oxone (400 mg, 1.3 mmol) in H_2O (4 mL) was added dropwise. The reaction was sealed under air and warmed to room temperature. After 20 h, the reaction was diluted with ice

water and extracted with ethyl acetate. The combined organic phases were washed with brine, dried over anhydrous magnesium sulfate, filtered, and concentrated under reduced pressure. The crude material was dissolved in DCM (5 mL). To this solution, imidazole (65 mg, 0.95 mmol) was added followed by TBSCl (130 mg, 0.85 mmol). The reaction was sealed under air at room temperature. After 3 h, the reaction was quenched by the addition of water and extracted with DCM. The combined organic phases were dried over anhydrous sodium sulfate, filtered, and concentrated under reduced pressure. This afforded the sulfone **32** (275 mg, 89%) as a white solid. ^{1}H NMR (500 MHz, $CDCl_3$) δ 9.07 (d, *J* = 5.2 Hz, 1H), 8.35 (d, *J* = 5.3, 1H), 5.40 – 5.27 (m, 1H), 4.91 (br, 2H), 4.31 (br, 2H), 3.42 (s, 3H), 3.01 (br, 2H), 2.26 (br, 4H), 1.49 (s, 9H), 0.92 (s, 9H), 0.10 (s, 6H). ^{13}C NMR (126 MHz, $CDCl_3$) δ 166.1, 159.7, 156.0, 154.6, 148.0, 130.4, 123.2, 80.0, 59.4, 55.9, 43.3, 39.2, 32.4, 30.3, 28.4, 25.7, -3.6. IR (NaCl, thin film, cm^{-1}): 2977, 2932, 1684, 1582, 1429, 1320, 1161, 1006, 736. HRMS (ESI): Calculated for $C_{24}H_{40}N_6NaO_5SSi^+$, $(M+Na)^+$ 575.2442, found 575.2430.

Synthesis of tert-butyl 4-(4-methyl-5-(2-(methylsulfonyl)pyrimidin-4-yl)-1H-1,2,3-triazol-1-yl)piperidine-1-carboxylate (33): The General Oxidation Procedure was used with thioether **30** and the sulfone was isolated in quantitative yield. ^{1}H NMR (400 MHz, $CDCl_3$) δ 9.02 (d, *J* = 5.3 Hz, 1H), 7.72 (d, *J* = 5.3 Hz, 1H), 5.35 – 5.06 (m, 1H), 4.26 (br, 2H), 3.37 (s, 3H), 2.94 (br, 2H), 2.58 (s, 3H), 2.36 – 2.09 (m, 4H), 1.45 (s, 9H). ^{13}C NMR (101 MHz, $CDCl_3$) δ 166.3, 159.3, 156.7, 154.6, 145.1, 128.4, 121.5, 79.8, 59.1, 42.8 (br), 39.2, 32.3, 28.4, 12.6. IR (NaCl, thin film, cm^{-1}): 2976, 2931, 1687, 1580, 1452, 1426, 1321, 1249, 1163, 1007. HRMS (ESI): Calculated for $C_{18}H_{26}N_6NaO_4S^+$, $(M+Na)^+$ 445.1628, found 445.1623.

General Nucleophilic Aromatic Substitution Procedure and Synthesis of tert-butyl 4-(5-(2-((3,5-dimethylphenyl)amino)pyrimidin-4-yl)-4-(4-fluorophenyl)-1H-1,2,3-triazol-1-

yl)piperidine-1-carboxylate (34): To a vial containing the sulfone **31** (85 mg, 0.170 mmol), 2,5-dimethylaniline (0.21 mL, 1.7 mmol) was added neat. The vial was sealed under air and heated to 100 °C. After 3 h, the reaction mixture was cooled to room temperature diluted with THF (0.5 mL) and then Boc_2O (0.10 mL, 0.44 mmol) was added. After an additional 2 h at room temperature, the reaction was concentrated under reduced pressure. Purification by column chromatography (0-60% IPA in hexanes with 1% TEA) yielded semi-pure material. The purified material was recrystallized in DCM and hexanes to afford the desired product **34** (54 mg, 59%) as a white solid. ^{1}H NMR (500 MHz, $CDCl_3$) δ 8.41 (d, J = 5.0 Hz, 1H), 7.59 (apparent dd, J = 8.7, 5.4 Hz, 2H), 7.36 (s, 1H), 7.20 (s, 2H), 7.10 (apparent t, J = 8.7 Hz, 2H), 6.80 (s, 1H), 6.61 (d, J = 5.0 Hz, 1H), 4.93 (tt, J = 11.4, 4.0 Hz, 1H), 4.16 (br, 2H), 2.58 (br, 2H), 2.33 (s, 6H), 2.32 – 2.19 (m, 2H), 2.09 – 2.02 (m, 2H), 1.49 (s, 9H). ^{13}C NMR (126 MHz, $CDCl_3$) δ 163.0 (d, J_{C-F} = 248.4 Hz), 160.7, 159.3, 156.0, 154.5, 145.7, 138.7, 138.3, 130.2 (d, J_{C-F} = 8.2 Hz), 130.0, 126.6 (d, J_{C-F} = 3.1 Hz), 125.7, 118.4, 115.8 (d, J_{C-F} = 21.7 Hz), 112.9, 79.9, 57.3, 42.7 (br), 32.2, 28.4, 21.4. ^{19}F NMR (376 MHz, $CDCl_3$) δ -112.7. IR (NaCl, thin film, cm^{-1}): 2974, 1691, 1536, 1430, 1160. HRMS (ESI): Calculated for $C_{30}H_{34}FN_7NaO_2^+$, $(M+Na)^+$ 566.2650, found 566.2643.

General Boc-Deprotection Procedure and Synthesis of N-(3,5-dimethylphenyl)-4-(4-(4-fluorophenyl)-1-(piperidin-4-yl)-1H-1,2,3-triazol-5-yl)pyrimidin-2-amine (VII): To a solution of the Boc protected amine **34** (18 mg, 32 μmol) in DCM (0.5 mL) at room temperature was added TFA (0.5 mL). After 1 h, the product was concentrated under reduced pressure. This afforded the product quantitatively as a yellow solid. The ratio of TFA and amine was determined by ^{19}F NMR. ^{1}H NMR (500 MHz, MeOD) δ 8.44 (d, J = 5.0 Hz, 1H), 7.60 (apparent dd, J = 8.8, 5.3 Hz, 2H), 7.27 – 7.18 (m, 4H), 6.79 (s, 1H), 6.68 (d, J = 5.0 Hz, 1H), 5.16 (tt, J = 10.7, 4.3 Hz, 1H), 3.52 – 3.45 (m, 2H), 2.96 – 2.86 (m, 2H), 2.55 – 2.36 (m, 4H), 2.31 (s, 6H).

^{13}C NMR (126 MHz, MeOD) δ 163.2 (d, J_{C-F} = 247.6 Hz), 160.8, 159.0, 155.2, 145.4, 139.0, 138.2, 130.9, 130.1 (d, J_{C-F} = 8.4 Hz), 126.2, 124.9, 118.9, 115.5 (d, J_{C-F} = 22.1 Hz), 112.0, 54.0, 42.7, 28.8, 20.1. ^{19}F NMR (376 MHz, MeOD) δ -77.5 (9 H), -114.3 (1H). IR (NaCl, thin film, cm^{-1}): 2916, 2850, 1676, 1624, 1592, 1510, 1457, 1198, 1186, 1160, 1143. HRMS (ESI): Calculated for $C_{25}H_{26}FN_7Na^+$, $(M+Na)^+$ 466.2126, found 466.2117. HPLC Purity: 96.3%.

Synthesis of tert-butyl 4-(4-(((tert-butyldimethylsilyl)oxy)methyl)-5-(2-((3,5-dimethylphenyl)amino)pyrimidin-4-yl)-1H-1,2,3-triazol-1-yl)piperidine-1-carboxylate (35): To a solution of 3,5-dimethylaniline (0.02 mL, 0.2 mmol) in THF (2 mL), cooled in a dry ice/acetone bath, was added NaHMDS (0.28 mL, 1 M in THF, 0.28 mmol). After 5 min, a solution of the sulfone **32** (62 mg, 0.11 mmol) in THF (2 mL) was added dropwise. After an additional 30 min, the reaction was quenched with water and extracted with ethyl acetate. The combined organic phases were washed with brine, dried over anhydrous sodium sulfate, filtered, and concentrated under reduced pressure. Purification by column chromatography (0-55% EtOAc in Hexanes) yielded the desired product **35** (39.1 mg, 59%) as a white solid. ^{1}H NMR (500 MHz, $CDCl_3$) δ 8.55 (d, J = 5.0 Hz, 1H), 7.40 (d, J = 5.0 Hz, 1H), 7.29 (s, 1H), 7.14 (s, 2H), 6.79 (s, 1H), 5.16 (tt, J = 11.3, 4.0 Hz, 1H), 4.87 (s, 2H), 4.11 (br, 2H), 2.51 (br, 2H), 2.32 (s, 6H), 2.24 – 2.15 (m, 2H), 2.07 – 1.96 (m, 2H), 1.48 (s, 9H), 0.91 (s, 9H), 0.13 (s, 6H). ^{13}C NMR (126 MHz, $CDCl_3$) δ 160.3, 159.4, 155.2, 154.5, 146.3, 138.6, 138.3, 132.3, 125.8, 118.9, 112.6, 79.8, 57.4, 56.9, 42.2, 32.1, 28.4, 25.9, 21.4, 18.3, -5.1. IR (NaCl, thin film, cm^{-1}): 2927, 2854, 1688, 1596, 1453, 1330, 1250, 1158. HRMS (ESI): Calculated for $C_{31}H_{47}N_7NaO_3Si^+$, $(M+Na)^+$ 616.3402, found 616.3394.

Synthesis of (5-(2-((3,5-dimethylphenyl)amino)pyrimidin-4-yl)-1-(piperidin-4-yl)-1H-1,2,3-triazol-4-yl)methanol (VIII): To a solution of the Boc protected amine **35** (39 mg, 66

μmol) in DCM (0.5 mL) at room temperature was added TFA (0.5 mL). After 3 h, the solution was heated to 40 °C. After 1 h, the reaction was concentrated under reduced pressure. Analysis by ^{19}F NMR with 2,2,2-trifluoroethanol as the standard indicated the formation of a mono TFA salt in quantitative yield. ^{1}H NMR (500 MHz, MeOD) δ 8.60 (d, J = 5.0 Hz, 1H), 7.31 (d, J = 5.0 Hz, 1H), 7.19 (s, 1H), 6.79 (s, 2H), 5.36 (tt, J = 10.8, 4.2 Hz, 1H), 4.79 (s, 2H), 3.44 (d, J = 13.2 Hz, 2H), 2.91 – 2.75 (m, 2H), 2.48 – 2.32 (m, 4H), 2.31 (s, 6H). ^{13}C NMR (126 MHz, MeOD) δ 160.8, 159.6, 154.3, 146.1, 139.1, 138.1, 132.6, 124.9, 119.3, 111.6, 54.4, 54.1, 42.7, 28.8, 20.1. IR (NaCl, thin film, cm^{-1}): 2932, 2859, 1679, 1627, 1595, 1463, 1403, 1190, 1139, 1076. HRMS (ESI): Calculated for $C_{20}H_{25}N_7NaO^+$, $(M+Na)^+$ 402.2013, found 402.2022. HPLC Purity: 96.9%.

Synthesis of tert-butyl 4-(5-(2-((3,5-dimethylphenyl)amino)pyrimidin-4-yl)-4-methyl-1H-1,2,3-triazol-1-yl)piperidine-1-carboxylate (36): A variation of the General SNAr procedure was used with sulfone **33**. The product was purified by prep TLC (20% IPA in Hexanes) and the product was isolated in 68% yield. ^{1}H NMR (500 MHz, $CDCl_3$) δ 8.54 (d, *J* = 5.0 Hz, 1H), 7.57 (s, 1H), 7.15 (s, 2H), 6.83 (d, *J* = 5.0 Hz, 1H), 6.78 (s, 1H), 5.06 (tt, *J* = 11.4, 4.0 Hz, 1H), 4.11 (s, 2H), 2.64 – 2.38 (m, 5H), 2.31 (s, 6H), 2.24 – 2.13 (m, 2H), 2.06 – 1.91 (m, 2H), 1.47 (s, 9H). ^{13}C NMR (126 MHz, $CDCl_3$) δ 160.5, 159.3, 155.7, 154.5, 143.3, 138.6, 138.4, 130.4, 125.7, 118.9, 111.5, 79.8, 57.2, 42.3 (br), 32.1, 28.4, 21.4, 12.0. IR (NaCl, thin film, cm^{-1}): 2974, 2929, 1693, 1567, 1537, 1427, 1366, 1164. HRMS (ESI): Calculated for $C_{25}H_{33}N_7NaO_2^+$, $(M+Na)^+$ 486.2588, found 486.2574.

Synthesis of N-(3,5-dimethylphenyl)-4-(4-methyl-1-(piperidin-4-yl)-1H-1,2,3-triazol-5-yl)pyrimidin-2-amine (IX): The general Boc deprotection procedure was used with Boc protected amine **36**, and the product was isolated in quantitative yield. Analysis by ^{19}F NMR with 2,2,2-trifluoroethanol as the standard indicated the formation of a bis-TFA salt in

quantitative yield. ^{1}H NMR (500 MHz, MeOD) δ 8.57 (d, *J* = 5.3 Hz, 1H), 7.18 (s, 2H), 7.07 (d, *J* = 5.3 Hz, 1H), 6.83 (s, 1H), 5.30 (tt, *J* = 10.7, 4.2 Hz, 1H), 3.43 (d, *J* = 13.3 Hz, 2H), 2.85 – 2.75 (m, 2H), 2.53 (s, 3H), 2.35 – 2.32 (m, 2H), 2.31 (s, 6H). ^{13}C NMR (126 MHz, MeOD) δ 159.8, 157.8, 155.8, 143.4, 138.5, 138.4, 130.8, 125.5, 119.7, 110.8, 54.2, 42.7, 28.7, 20.1, 10.4. IR (NaCl, thin film, cm^{-1}): 2925, 2852, 1681, 1628, 1593, 1513, 1460, 1198, 1141. HRMS (ESI): Calculated for $C_{20}H_{25}N_7Na^+$, $(M+Na)^+$ 386.2064, found 386.2053. HPLC Purity: 96.1%.

Scheme 6: Synthesis of Fluorescein-JQ1 Tracer (**40**)

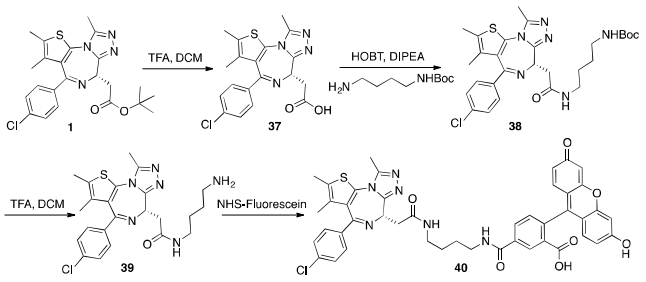

Synthesis of (S)-N-(4-aminobutyl)-2-(4-(4-chlorophenyl)-2,3,9-trimethyl-6H-thieno[3,2-f][1,2,4]triazolo[4,3-a][1,4]diazepin-6-yl)acetamide (39): Commercially acquired (+)-JQ1 (Sigma, SML0974) was hydrolyzed to the acid **37**, conjugated to the N-Boc-1,4-butanediamine linker (Sigma, 15404), and deprotected to yield the free amine **39** according to previously reported procedures.[53]

Synthesis of (S)-5-((4-(2-(4-(4-chlorophenyl)-2,3,9-trimethyl-6H-thieno[3,2-f][1,2,4]triazolo[4,3-a][1,4]diazepin-6-yl)acetamido)butyl)carbamoyl)-2-(6-hydroxy-3-oxo-3H-xanthen-9-yl)benzoic acid (40): To a solution of **39** (8 mg, 12 μmol) in DCM (1 mL), was added NHS-Fluorescein (6 mg, 13 mmol; Thermo Scientific, 46409). The reaction mixture was stirred overnight at room temperature and purified using reverse-phase chromatography. HRMS (ESI): Calculated for $C_{44}H_{37}ClN_6O_7S$ $(M+H)^+$ 829.3250, found 829.3762; $C_{44}H_{37}ClN_6NaO_7S$ $(M+Na)^+$ 851.2031, found 851.3621.

Protein Expression: Expression of BRD4(1), BRD4(2), H437D BRD4(2), BRD4(1+2), BRDT(1), BRDT(2), BPTF, and 5FW-pfGCN5 in either unlabeled or 5FW labeled forms was based on established methods using *E. coli* Bl21(DE3) + pRARE strains,[26] and is briefly described here. To express the labeled protein, the secondary culture in LB media was grown until an O.D. at 600 nm of 0.6 was reached followed by harvesting. Cells were resuspended in defined media containing 5-fluoroindole (60 mg/L) in place of tryptophan. The resuspended *E. coli* were incubated at 37 °C while shaking for 1.5 h. followed by cooling to 20 °C and media temperature equilibration for 30 min. Protein expression was induced with 1 mM IPTG overnight (14−16 h) at 20 °C. The cells were harvested and stored at −20 °C. Cell pellets were thawed at room temperature followed by the addition of lysis buffer (50 mM potassium phosphate pH 7.4, 300 mM NaCl) containing protease inhibitor PMSF (5 mM) + Halt protease inhibitor cocktail, and purified using Ni-affinity chromatography. Purity of proteins was assessed by SDS-PAGE. Fluorinated amino acid incorporation efficiency in proteins was measured by LC-MS on a Waters Synapt G2 UPLC/QTOF-MS. Protein concentrations were determined via absorbance at 280 nm.

Fluorescence Anisotropy: Fluorescence anisotropy experiments were carried out in 50 mM HEPES, 100 mM NaCl, 4 mM CHAPS, pH 7.4 on 384-well plates (Corning 4511). 25 μM stock solutions of fluorescent tracer in DMSO were diluted to 15 nM for these experiments. Plates were read on a Tecan Infinity 500 with an excitation wavelength at 485 nm and emission at 535 nm. For direct binding experiments, the protein was serially diluted across the plate, and the resulting anisotropy values were fit using Equation 1 in GraphPad Prism, where b and c are the maximum and minimum anisotropy values, respectively, a is the concentration of fluorescent tracer, x is the concentration of protein, and y is the observed anisotropy value.

$$y = c + (b - c)\frac{(K_d + a + x) - \sqrt{(K_d + a + x)^2 - 4ax}}{2a} \quad \text{(Equation 1)}$$

The protein concentration for competition experiments was determined from the protein concentration in direct binding experiments at which the fluorescent tracer is 80% bound. Stock solutions of inhibitor molecules, which are 50 mM in DMSO, were serially diluted from 250 μM to subnanomolar concentrations, keeping the concentration of protein, tracer, and other components constant. Anisotropy values were fit using GraphPad Prism's log(inhibitor) vs. response (four parameters) function. The IC_{50} values are reported as the Mean ± SEM, determined from three or more independent experiments. Direct binding with fluorescent tracer and self-competition experiments with JQ1 or BI-2536 were carried out prior to each set of competition experiments to assess protein quality, assay stability and for determination of percent bound for those compounds that did not show complete inhibition.

Isothermal Titration Calorimetry: To measure the interaction parameters with BRD4(1) we used a GE Auto ITC200. 35 μM of BRD4(1) and varying concentrations of compounds **IV** and **V** were used for all the experiments. BRD4(1) solution was loaded in the sample cell of the calorimeter and titrated with solutions of **IV** or **V**. 50 mM potassium phosphate at pH 7.5 containing 150 mM NaCl was used to dilute stock solution of both compounds and protein. Diluted solutions of protein were concentrated in a 3 kDa cutoff centrifuge filter. **IV** or **V** were diluted from a 50 mM stock solution in DMSO into the same buffer as protein to the required concentration, briefly sonicated, and used for the titration. Titrations were carried out by injecting 1 μL followed by 20 identical injections of 2 μL with a releasing period of 5 seconds per injection every 300 seconds. Control heat of dilution was measured by independent ligand titration into buffer and was subtracted from the protein-ligand binding experimental data. Data was analyzed by Origin™ software to calculate enthalpy of binding (ΔH) and association

constants (K_a). Heat liberated by each injection was integrated (ΔH) and plotted against molar ratio of ligand and protein.

Protein Observed Fluorine NMR: ^{19}F NMR spectra were acquired at 470 MHz on a Bruker 500 spectrometer with a 5 mm Prodigy TCI Cryoprobe without proton decoupling. Samples containing 40−50 μM bromodomains were dosed in 50 mM TRIS, 100 mM NaCl, and 5% D_2O, pH 7.4 with varying ligand concentrations for binding assays and normalized to 0.05% DMSO. Spectra were referenced to trifluoroacetate (−76.55 ppm). Measurement parameters included a relaxation delay time of 0.7 s and a 90° flip angle. An acquisition time of 0.05 s was used for all experiments. A spectral width of at least 10 ppm was used for all spectra and screening experiments used 400 transients.

Site-Directed Mutagenesis: Site-directed mutagenesis of H437D on BRD4(2) was conducted using previously reported transfer-PCR procedures in 50 μL reaction mixtures.[54] Reaction mixtures contained Phusion High-Fidelity Master Mix (NEB), template DNA, 50 nM each of the T7-forward primer (5'- TAATACGACTCACTATAGGG-3') and reverse complement primer (5'- CAACCCTCCTGACG*ATGAGGTGGTGGC-3', where * indicates site of mutation). Successful mutagenesis was confirmed by DNA sequencing.

X-Ray Crystallography: Crystals of BRD4-1 were grown in the presence of 1 mM ligand and 10% (v/v) DMSO from vapor-diffusion hanging drops from 0.1 M $(NH4)_2SO_4$, 0.05 M Tris (pH 8.5) and 12.5 % (w/v) PEG 3350 as described previously.[25] Crystals were flash frozen in a stream of nitrogen gas and X-ray diffraction data were recorded at -180 °C at beamline X11 of the Advanced Photon Source, Argonne National Laboratories. Data were reduced and scaled with XDS;[55] PHENIX[56] was employed for phasing and refinement, and model building was performed using Coot.[57] All structures were solved by molecular replacement using PDB entry

4O7B[25] as the search model. Initial models for the small molecule ligands were generated using MarvinSketch (ChemAxon, Cambridge, MA) with ligand restraints from eLBOW of the PHENIX suite. Figures were prepared using PyMOL (Schrödinger, LLC).

Cell Culture: MM.1S and A549-NF-κB-luc cells were grown in a humidified 5% CO_2 environment at 37 °C. A549-NF-κB-luc cells[58] were cultured in DMEM media (Gibco) supplemented with 10% fetal bovine serum (FBS, Cellgro) penicillin (50 I.U./mL, Cellgro), streptomycin (50 µg/mL, Cellgro) and hygromycin (100 µg/mL, Roche). Cells were maintained at a density below 2×10^6 cells/mL and dissociated from adherent plates in 0.25% trypsin/EDTA (Gibco) with 2 min. incubation times. MM.1S cells were grown in RPMI-1640 containing 10% FBS. Cell line authenticity was verified using the Short Tandem Repeat (STR) profiling service provided by ATCC.

Western Blotting: MM.1S cells were seeded in 6-well plates at a density of 10^6 cells per well and exposed to increasing compound concentrations ranging from 0.1 to 30 µM for 6 h. Cells were harvested by low speed centrifugation at 300 X g for 5 min and washed once with PBS. Cells were lysed in 75 µl CelLytic M (Sigma Aldrich, St. Louis, MO) supplemented with 1X Halt Protease and Phosphatase Inhibitor Cocktail and 5 mM EDT (ThermoFisher Scientific, Carlsbad, CA). Protein concentration was assessed with the Bio-Rad Protein Assay Dye Reagent, and samples were mixed with 1/3 vol of 4X SDS sample buffer (Bio-Rad) containing 10% β-mercaptoethanol, followed by 12.5% SDS-PAGE. Proteins were transferred to PVDF membranes for 3 h on ice using Bio-Rad Mini Trans-Blot Cells. Membranes were incubated with TBS-T containing 5% non-fat dry milk for 1 h at room temperature, followed by a 16 h incubation with primary antibodies (c-Myc, Cell Signaling Technology, #5605, diluted 1:4,000 in TBS-T containing 5% BSA; GAPDH, BioLegend #919501, diluted 1:50,000 in TBS-T

containing 5% non-fat dry milk) at 4˚C. After washing the membranes 3X with TBS-T, they were incubated with 1,000-fold diluted HRP-conjugated secondary antibodies from Jackson ImmunoResearch (Goat Anti-Rabbit IgG, #111-035-003 and Goat Anti-Mouse IgG, #115-035-003). Membranes were again washed 3X with TBS-T and then exposed to SignalFire ECL Reagent (Cell Signaling Technology) for 1 min, followed by exposure to X-ray film.

Viability Assays: MM.1S cells were seeded in 96-well plates at approximately 20,000 cells per well (0.1 ml) and incubated with increasing compound concentrations in the presence of 0.1% DMSO for 72 h with 6 replicates per concentration. After drug treatment, 15 µl of CellTiter Blue reagent (Promega) was added to each well, followed by vigorous orbital shaking for 5 min and incubation for 3 h at 37 ºC. Plates were placed in a Wallac EnVision 2103 Multilabel Reader (PerkinElmer), and fluorescence was determined using excitation and emission filters of 570 nm and 615 nm, respectively. Dose-response data were analyzed with GraphPad Prism.

Cellular Thermal Shift Assay: Assays were performed as previously reported by Jafari et al.[37] in both the isothermal dose-response and melt curve formats. 1 x 10^6 cells were treated with desired amounts of compound, with DMSO concentrations normalized to 0.1% for all samples. Dosed cells were incubated in DMEM media at 37 °C for 1 hour with mild intermittent agitation. Upon completion of the incubation period, cells were thermally denatured for 3 minutes in a heated water bath and subsequently equilibrated at room temperature for a further 3 minutes. Following centrifugation and rinsing with PBS, cells were lysed over three freeze thaw cycles before soluble protein concentrations of supernatant were determined using the BCA protein assay kit (Pierce). Samples were normalized to the lowest total soluble protein concentration amongst grouped samples.

NuPAGE 4X LDS sample buffer and NuPAGE 10X sample reducing agent (Invitrogen) were added to normalized protein samples and denatured by heating at 90 °C for 5 minutes. Protein samples were separated on a gradient 4-12% SDS-PAGE gel (Invitrogen), transferred to a polyvinylidene difluoride membrane (Immobilon) and blocked by incubating in blocking buffer (0.05 g/mL BioRad Non-fat milk in PBS) at 4 °C overnight. Proteins were detected by incubation with primary antibodies (BRD4 Rabbit mAb: Cell Signaling Technologies, 13440; p38α Rabbit mAb: Cell Signaling Technologies, 9212 and β-actin Mouse mAb: Santa Cruz Biotechnology, SC-47778) diluted 1:1000 in blocking buffer for 4 h. at room temperature. The membrane was washed in MQ-water and incubated with HRP-conjugate anti-mouse (Thermo, A16066) or anti-rabbit secondary antibodies (Thermo, 65-6120) similarly diluted in blocking buffer, for 1 h. at room temperature. The membrane was again washed in MQ-water before immunocomplexes were visualized upon addition of HRP substrate (Thermo) using the Odyssey FC imaging system (LICOR Biotech.).

NF-κB Reporter Assay: Reporter assays were performed as previously described by Hexum et al.[58] Briefly, compounds were serially diluted and dosed to A549-NF-κB-luc cells (final volume/well = 100 μL; final DMSO concentration = 0.5%) in 96-well plates. NF-κB was induced by the addition of TNF-α (15 ng/mL final concentration, diluted in PBS; Invitrogen) 30 minutes after dosing. Bright-Glo luciferase reagent (Promega) was added to each well (100 μL) after 8 h. and luminescence measurements were obtained on a Synergy plate reader. Cellular viability was measured in parallel by colorimetric viability staining (Alamar Blue, Invitrogen). Cell viabilities of compound treated cells is shown in Fig.S14.

Data is reported as Mean ± SEM from three replicate biological experiments with three technical replicates per experiment. Mean and uncertainty in each % NF-κB activity value was

calculated by propagating the calculated means from individual biological replicates. Statistical analyses and plotting of results were performed on GraphPad Prism (v. 7.0).

IL-8 ELISA: A549-NF-κB-luc cells were seeded into 24-well plates at a cell density of 2×10^5 cells/well. Cells were incubated with compounds for 24 hours, where cells were induced with TNF-α (10 ng/mL) 6 h after the initial dosing, resulting in an 18 h induction. Upon completion of the incubation period, cell media (500 μL) was harvested and centrifuged (10,000 X g, 5 min.) before secreted IL-8 protein levels were measured using a human IL-8 ELISA kit (Thermo Scientific, EH2IL8) following vendor instructions. On a Synergy plate reader, the absorbance of each sample at 450 nm and 550 nm was collected following addition of the substrate stop solution. A standard curve was plotted in Microsoft Excel and $A_{450\text{-}550}$ values of unknown samples were plotted against the standard curve to yield IL-8 protein concentrations in pg/mL.

Data is reported as Mean ± SEM from three replicate biological experiments with three technical replicates per experiment. Mean and uncertainty in each IL-8 concentration value was calculated by propagating the calculated means from individual biological replicates. Statistical analyses and plotting of results were performed on GraphPad Prism (v. 7.0).

ABBREVIATIONS USED

BET, Bromodomain and Extra Terminal; BRD4, Bromodomain-containing protein 4; BRD2, Bromodomain-containing protein 2; BRD3, Bromodomain-containing protein 3; BRDT, Bromodomain testis-specific protein; c-Myc, Myc proto-oncogene protein; NF-κB, nuclear factor κ-light-chain-enhancer of activated B cells; IL-8, Interleukin-8; K_{ac}, N-ε-acetylated-lysine; D1, N-terminal BET bromodomain; D2, C-terminal BET bromodomain; dTAG, degradation tag; p38α, Mitogen-activated protein kinase 14; BPTF, Nucleosome-remodeling factor subunit BPTF; DSF, Differential Scanning Fluorimetry; FA, Fluorescence Anisotropy; ITC, Isothermal

Titration Calorimetry; ALPHAScreen, Amplified Luminescent Proximity Homogeneous Assay; PrOF NMR, Protein-observed fluorine NMR; GCN5, Histone acetyltransferase GCN5; TRIM24, Transcription intermediary factor 1-alpha; SMARCA2, Probable global transcription activator SNF2L2; PCAF, Histone acetyltransferase KAT2B; p300, Histone acetyltransferase p300; SMARCA4, Transcription activator BRG1; MAP, Mitogen-Activated Protein; GAPDH, Glyceraldehyde-3-phosphate dehydrogenase; CETSA, CEllular Thermal Shift Assay; MSK1, Ribosomal protein S6 kinase alpha-5; TR-FRET, Time-Resolved Förster Resonance Energy Transfer; CSBP, Mitogen-activated protein kinase 14; DAD, Diode-Array Detector; CSA, Camphorulfonic Acid; DMF-DMA, N,N-Dimethylformamide-dimethylacetal; TLC, Thin-Layer Chromatography; THF, Tetrahydrofuran; IPA, Isopropyl Alcohol; DCM, Dichloromethane; NaHMDS, Sodium bis(trimethylsilyl)amide; NHS, N-Hydroxysuccinimide; IPTG, Isopropyl β-D-1-thiogalactopyranoside; PMSF, phenylmethylsulfonyl fluoride; SDS-PAGE, sodium dodecyl sulfate–polyacrylamide gel electrophoresis; QTOF-MS, quadrupole time-of-flight mass spectrometery; HEPES, 4-(2-hydroxyethyl)-1-piperazineethanesulfonic acid); CHAPS, 3-[(3-Cholamidopropyl)dimethylammonio]-1-Propanesulfonate; FBS, Fetal Bovine Serum; EDT, Ethanedithiol.

ASSOCIATED CONTENT

Supporting Information. Authors will release the atomic coordinates and crystallographic data for PDB Codes 6MH1 and 6MH7 upon article publication. The following files are available free of charge:

Supporting Information (PDF)

NMR Spectra of Compounds Synthesized (PDF)

Molecular String Files for Final Compounds Synthesized (CSV)

AUTHOR INFORMATION

Corresponding Author

*Email: wcp@umn.edu and daharki@umn.edu.

Author Contributions

S.K.T. designed and synthesized molecules with H.C.; A.M.A. and N.K.M. performed biophysical experiments; A.D., J.C.W. and N.B. designed and performed cellular experiments; J.Y.Z. performed crystallography; D.A.H and W.C.K.P oversaw the experimental and interpretation of data. A.D. and W. C. K. P. wrote the manuscript. All authors have given approval to the final version of the manuscript. ‡These authors contributed equally.

Funding Sources

This work was supported by the NSF (Grant CHE-1352019, W.C.K.P.), AHA (Grant 15SDG25710427, W.C.K.P.), NIGMS (Grant R35GM124718) and the University of Minnesota Masonic Cancer Center (Pre-R01 pilot grant, D.A.H. and W.C.K.P.) A.D. was supported by the NIH chemistry–biology interface training grant at the University of Minnesota (5T32GM008700-18).

ACKNOWLEDGMENT

Isothermal titration calorimetry and Nuclear Magnetic Resonance spectroscopy were carried out using instruments funded by NIH Shared Instrumentation Grants (S10-OD017982 and S10-OD011952, respectively). We also thank the Moffitt Chemical Biology Core for use of the protein crystallography facility (NCI Grant P30-CA076292). A.D. acknowledges the NIH

Chemistry-Biology Interface Training Grant (5T32GM008700). BI-BODIPY was a generous gift from Wei Zhang at the University of Massachusetts, Boston.

REFERENCES

(1) Allfrey, V. G.; Faulkner, R.; Mirsky, A. E. Acetylation and Methylation of Histones and Their Possible Role in the Regulation of Rna Synthesis. *Proc. Natl. Acad. Sci.* **1964**, *51* (1938), 786–794.

(2) Bannister, A. J.; Kouzarides, T. Regulation of Chromatin by Histone Modifications. *Cell Res.* **2011**, *21* (3), 381–395.

(3) Muller, S.; Filippakopoulos, P.; Knapp, S. Bromodomains as Therapeutic Targets. *Expert Rev. Mol. Med.* **2011**, *13* (September), e29.

(4) Fujisawa, T.; Filippakopoulos, P. Functions of Bromodomain-Containing Proteins and Their Roles in Homeostasis and Cancer. *Nat. Rev. Mol. Cell Biol.* **2017**, *18* (4), 246–262.

(5) Filippakopoulos, P.; Knapp, S. The Bromodomain Interaction Module. *FEBS Lett.* **2012**, *586* (17), 2692–2704.

(6) Filippakopoulos, P.; Qi, J.; Picaud, S.; Shen, Y.; Smith, W. B.; Fedorov, O.; Morse, E. M.; Keates, T.; Hickman, T. T.; Felletar, I.; Philpott, M.; Munro, S.; McKeown, M. R.; Wang, Y.; Christie, A. L.; West, N.; Cameron, M. J.; Schwartz, B.; Heightman, T. D.; La Thangue, N.; French, C. A.; Wiest, O.; Kung, A. L.; Knapp, S.; Bradner, J. E. Selective Inhibition of BET Bromodomains. *Nature* **2010**, *468* (7327), 1067–1073.

(7) Huang, B.; Yang, X.-D.; Zhou, M.-M.; Ozato, K.; Chen, L.-F. Brd4 Coactivates

Transcriptional Activation of NF-KappaB via Specific Binding to Acetylated RelA. *Mol. Cel. Biol.* **2009**, *29* (5), 1375–1387.

(8) Lovén, J.; Hoke, H. A.; Lin, C. Y.; Lau, A.; Orlando, D. A.; Vakoc, C. R.; Bradner, J. E.; Lee, T. I.; Young, R. A. Selective Inhibition of Tumor Oncogenes by Disruption of Super-Enhancers. *Cell* **2013**, *153* (2), 320–334.

(9) Filippakopoulos, P.; Picaud, S.; Mangos, M.; Keates, T.; Lambert, J. P.; Barsyte-Lovejoy, D.; Felletar, I.; Volkmer, R.; Müller, S.; Pawson, T.; Gingras, A. C.; Arrowsmith, C. H.; Knapp, S. Histone Recognition and Large-Scale Structural Analysis of the Human Bromodomain Family. *Cell* **2012**, *149* (1), 214–231.

(10) Ouyang, L.; Zhang, L.; Liu, J.; Fu, L.; Yao, D.; Zhao, Y.; Zhang, S.; Wang, G.; He, G.; Liu, B. Discovery of a Small-Molecule Bromodomain-Containing Protein 4 (BRD4) Inhibitor That Induces AMP-Activated Protein Kinase-Modulated Autophagy-Associated Cell Death in Breast Cancer. *J. Med. Chem.* **2017**, *60* (24), 9990–10012.

(11) Brand, M.; Measures, A. M.; Wilson, B. G.; Cortopassi, W. A.; Alexander, R.; Höss, M.; Hewings, D. S.; Rooney, T. P. C.; Paton, R. S.; Conway, S. J. Small Molecule Inhibitors of Bromodomain–Acetyl-Lysine Interactions. *ACS Chem. Biol.* **2015**, *10* (1), 22–39.

(12) Andrieu, G.; Belkina, A. C.; Denis, G. V. Clinical Trials for BET Inhibitors Run Ahead of the Science. *Drug Discov. Today Technol.* **2016**, *19*, 45–50.

(13) Amorim, S.; Stathis, A.; Gleeson, M.; Iyengar, S.; Magarotto, V.; Leleu, X.; Morschhauser, F.; Karlin, L.; Broussais, F.; Rezai, K.; Herait, P.; Kahatt, C.; Lokiec, F.; Salles, G.; Facon, T.; Palumbo, A.; Cunningham, D.; Zucca, E.; Thieblemont, C.

Bromodomain Inhibitor OTX015 in Patients with Lymphoma or Multiple Myeloma: A Dose-Escalation, Open-Label, Pharmacokinetic, Phase 1 Study. *Lancet Haematol.* **2016**, *3* (4), e196–e204.

(14) Picaud, S.; Wells, C.; Felletar, I.; Brotherton, D.; Martin, S.; Savitsky, P.; Diez-Dacal, B.; Philpott, M.; Bountra, C.; Lingard, H.; Fedorov, O.; Muller, S.; Brennan, P. E.; Knapp, S.; Filippakopoulos, P. RVX-208, an Inhibitor of BET Transcriptional Regulators with Selectivity for the Second Bromodomain. *Proc. Natl. Acad. Sci.* **2013**, *110* (49), 19754–19759.

(15) Kharenko, O. A.; Gesner, E. M.; Patel, R. G.; Norek, K.; White, A.; Fontano, E.; Suto, R. K.; Young, P. R.; McLure, K. G.; Hansen, H. C. RVX-297- a Novel BD2 Selective Inhibitor of BET Bromodomains. *Biochem. Biophys. Res. Commun.* **2016**, *477* (1), 62–67.

(16) Berkovits, B. D.; Wolgemuth, D. J. The First Bromodomain of the Testis-Specific Double Bromodomain Protein Brdt Is Required for Chromocenter Organization That Is Modulated by Genetic Background. *Dev. Biol.* **2011**, *360* (2), 358–368.

(17) Philpott, M.; Rogers, C. M.; Yapp, C.; Wells, C.; Lambert, J. P.; Strain-Damerell, C.; Burgess-Brown, N. A.; Gingras, A. C.; Knapp, S.; Müller, S. Assessing Cellular Efficacy of Bromodomain Inhibitors Using Fluorescence Recovery after Photobleaching. *Epigenetics and Chromatin* **2014**, *7* (1), 14.

(18) Zou, Z.; Huang, B.; Wu, X.; Zhang, H.; Qi, J.; Bradner, J.; Nair, S.; Chen, L. F. Brd4 Maintains Constitutively Active NF-KB in Cancer Cells by Binding to Acetylated RelA. *Oncogene* **2014**, *33* (18), 2395–2404.

(19) Zhang, G.; Plotnikov, A. N.; Rusinova, E.; Shen, T.; Morohashi, K.; Joshua, J.; Zeng, L.; Mujtaba, S.; Ohlmeyer, M.; Zhou, M. M. Structure-Guided Design of Potent Diazobenzene Inhibitors for the BET Bromodomains. *J. Med. Chem.* **2013**, *56* (22), 9251–9264.

(20) Hewings, D. S.; Wang, M.; Philpott, M.; Fedorov, O.; Uttarkar, S.; Filippakopoulos, P.; Picaud, S.; Vuppusetty, C.; Marsden, B.; Knapp, S.; Conway, S. J.; Heightman, T. D. 3,5-Dimethylisoxazoles Act as Acetyl-Lysine-Mimetic Bromodomain Ligands. *J. Med. Chem.* **2011**, *54* (19), 6761–6770.

(21) Gacias, M.; Gerona-Navarro, G.; Plotnikov, A. N.; Zhang, G.; Zeng, L.; Kaur, J.; Moy, G.; Rusinova, E.; Rodriguez, Y.; Matikainen, B.; Vincek, A.; Joshua, J.; Casaccia, P.; Zhou, M. M. Selective Chemical Modulation of Gene Transcription Favors Oligodendrocyte Lineage Progression. *Chem. Biol.* **2014**, *21* (7), 841–854.

(22) Baud, M. G. J.; Lin-Shiao, E.; Cardote, T.; Tallant, C.; Pschibul, A.; Chan, K.-H.; Zengerle, M.; Garcia, J. R.; Kwan, T. T.-L.; Ferguson, F. M.; Ciulli, A. Chemical Biology. A Bump-and-Hole Approach to Engineer Controlled Selectivity of BET Bromodomain Chemical Probes. *Science* **2014**, *346* (6209), 638–641.

(23) Runcie, A. C.; Zengerle, M.; Chan, K. H.; Testa, A.; Van Beurden, L.; Baud, M. G. J.; Epemolu, O.; Ellis, L. C. J.; Read, K. D.; Coulthard, V.; Brien, A.; Ciulli, A. Optimization of a "Bump-and-Hole" Approach to Allele-Selective BET Bromodomain Inhibition. *Chem. Sci.* **2018**, *9* (9), 2452–2468.

(24) Elkins, J. M.; Fedele, V.; Szklarz, M.; Abdul Azeez, K. R.; Salah, E.; Mikolajczyk, J.;

Romanov, S.; Sepetov, N.; Huang, X.-P.; Roth, B. L.; Al Haj Zen, A.; Fourches, D.; Muratov, E.; Tropsha, A.; Morris, J.; Teicher, B. A.; Kunkel, M.; Polley, E.; Lackey, K. E.; Atkinson, F. L.; Overington, J. P.; Bamborough, P.; Müller, S.; Price, D. J.; Willson, T. M.; Drewry, D. H.; Knapp, S.; Zuercher, W. J. Comprehensive Characterization of the Published Kinase Inhibitor Set. *Nat. Biotechnol.* **2016**, *34* (1), 95–103.

(25) Ember, S. W. J.; Zhu, J. Y.; Olesen, S. H.; Martin, M. P.; Becker, A.; Berndt, N.; Georg, G. I.; Schonbrunn, E. Acetyl-Lysine Binding Site of Bromodomain-Containing Protein 4 (BRD4) Interacts with Diverse Kinase Inhibitors. *ACS Chem. Biol.* **2014**, *9* (5), 1160–1171.

(26) Urick, A. K.; Hawk, L. M. L.; Cassel, M. K.; Mishra, N. K.; Liu, S.; Adhikari, N.; Zhang, W.; Dos Santos, C. O.; Hall, J. L.; Pomerantz, W. C. K. Dual Screening of BPTF and Brd4 Using Protein-Observed Fluorine NMR Uncovers New Bromodomain Probe Molecules. *ACS Chem. Biol.* **2015**, *10* (10), 2246–2256.

(27) Boehm, J. C.; Bower, M. J.; Gallagher, T. F.; Kassis, S.; Johnson, S. R.; Adams, J. L. Phenoxypyrimidine Inhibitors of P38α Kinase: Synthesis and Statistical Evaluation of the P38 Inhibitory Potencies of a Series of 1-(Piperidin-4-Yl)-4-(4-Fluorophenyl)-5-(2-Phenoxypyrimidin-4-Yl) Imidazoles. *Bioorganic Med. Chem. Lett.* **2001**, *11* (9), 1123–1126.

(28) Ciceri, P.; Müller, S.; O'Mahony, A.; Fedorov, O.; Filippakopoulos, P.; Hunt, J. P.; Lasater, E. A.; Pallares, G.; Picaud, S.; Wells, C.; Martin, S.; Wodicka, L. M.; Shah, N. P.; Treiber, D. K.; Knapp, S. Dual Kinase-Bromodomain Inhibitors for Rationally Designed Polypharmacology. *Nat. Chem. Biol.* **2014**, *10* (4), 305–312.

(29) Philpott, M.; Yang, J.; Tumber, T.; Fedorov, O.; Uttarkar, S.; Filippakopoulos, P.; Picaud, S.; Keates, T.; Felletar, I.; Ciulli, A.; Knapp, S.; Heightman, T. D. Bromodomain-Peptide Displacement Assays for Interactome Mapping and Inhibitor Discovery. *Mol. Biosyst.* **2011**, *7* (10), 2899.

(30) Mishra, N. K.; Urick, A. K.; Ember, S. W. J.; Schonbrunn, E.; Pomerantz, W. C. Fluorinated Aromatic Amino Acids Are Sensitive 19f NMR Probes for Bromodomain-Ligand Interactions. *ACS Chem. Biol.* **2014**, *9* (12), 2755–2760.

(31) Arntson, K. E.; Pomerantz, W. C. K. Protein-Observed Fluorine NMR: A Bioorthogonal Approach for Small Molecule Discovery. *J. Med. Chem.* **2016**, *59* (11), 5158–5171.

(32) Ishima, R.; Torchia, D. A. Protein Dynamics from NMR. *Nat. Struct. Biol.* **2000**, *7* (9), 740–743.

(33) Aldeghi, M.; Ross, G. A.; Bodkin, M. J.; Essex, J. W.; Knapp, S.; Biggin, P. C. Large-Scale Analysis of Water Stability in Bromodomain Binding Pockets with Grand Canonical Monte Carlo. *Commun. Chem.* **2018**, *1* (1), 19.

(34) Bharatham, N.; Slavish, P. J.; Young, B. M.; Shelat, A. A. The Role of ZA Channel Water-Mediated Interactions in the Design of Bromodomain-Selective BET Inhibitors. *J. Mol. Graph. Model.* **2018**, *81*, 197–210.

(35) Liu, J.; Li, F.; Bao, H.; Jiang, Y.; Zhang, S.; Ma, R.; Gao, J.; Wu, J.; Ruan, K. The Polar Warhead of a TRIM24 Bromodomain Inhibitor Rearranges a Water-Mediated Interaction Network. *FEBS J.* **2017**, *284* (7), 1082–1095.

(36) Wang, Z.; Canagarajah, B. J.; Boehm, J. C.; Kassisà, S.; Cobb, M. H.; Young, P. R.; Abdel-Meguid, S.; Adams, J. L.; Goldsmith, E. J. Structural Basis of Inhibitor Selectivity in MAP Kinases. *Structure* **1998**, *6* (9), 1117–1128.

(37) Jafari, R.; Almqvist, H.; Axelsson, H.; Ignatushchenko, M.; Lundbäck, T.; Nordlund, P.; Molina, D. M. The Cellular Thermal Shift Assay for Evaluating Drug Target Interactions in Cells. *Nat. Protoc.* **2014**, *9* (9), 2100–2122.

(38) Tanaka, M.; Roberts, J. M.; Seo, H.-S.; Souza, A.; Paulk, J.; Scott, T. G.; DeAngelo, S. L.; Dhe-Paganon, S.; Bradner, J. E. Design and Characterization of Bivalent BET Inhibitors. *Nat. Chem. Biol.* **2016**, *12* (12), 1089–1096.

(39) Martinez Molina, D.; Jafari, R.; Ignatushchenko, M.; Seki, T.; Larsson, E. A.; Dan, C.; Sreekumar, L.; Cao, Y.; Nordlund, P. Monitoring Drug Target Engagement in Cells and Tissues Using the Cellular Thermal Shift Assay. *Science (80-.).* **2013**, *341* (6141), 84–87.

(40) Huang, F.; Shao, W.; Fujinaga, K.; Peterlin, B. M. Bromodomain-Containing Protein 4 – Independent Transcriptional Activation by Autoimmune Regulator (AIRE) and NF-KB. *J. Biol. Chem.* **2018**, *293* (14), 4993–5004.

(41) Jung, M.; Philpott, M.; Müller, S.; Schulze, J.; Badock, V.; Eberspächer, U.; Moosmayer, D.; Bader, B.; Schmees, N.; Fernández-Montalván, A.; Haendler, B. Affinity Map of Bromodomain Protein 4 (BRD4) Interactions with the Histone H4 Tail and the Small Molecule Inhibitor JQ1. *J. Biol. Chem.* **2014**, *289* (13), 9304–9319.

(42) Harada, A.; Sekido, N.; Akahoshi, T.; Wada, T.; Mukaida, N.; Matsushima, K. Essential Involvement of Interleukin-8 (IL-8) in Acute Inflammation. *J. Leukoc. Biol.* **1994**, *56* (5),

559–564.

(43) Wen, B.; Hexum, J. K.; Widen, J. C.; Harki, D. A.; Brummond, K. M. A Redox Economical Synthesis of Bioactive 6,12-Guaianolides. *Org. Lett.* **2013**, *15* (11), 2644–2647.

(44) Nicodeme, E.; Jeffrey, K. L.; Schaefer, U.; Beinke, S.; Dewell, S.; Chung, C. W.; Chandwani, R.; Marazzi, I.; Wilson, P.; Coste, H.; White, J.; Kirilovsky, J.; Rice, C. M.; Lora, J. M.; Prinjha, R. K.; Lee, K.; Tarakhovsky, A. Suppression of Inflammation by a Synthetic Histone Mimic. *Nature* **2010**, *468* (7327), 1119–1123.

(45) Belkina, A. C.; Nikolajczyk, B. S.; Denis, G. V. BET Protein Function Is Required for Inflammation: Brd2 Genetic Disruption and BET Inhibitor JQ1 Impair Mouse Macrophage Inflammatory Responses. *J. Immunol.* **2013**, *190* (7), 3670–3678.

(46) Milletti, F.; Hermann, J. C. Targeted Kinase Selectivity from Kinase Profiling Data. *ACS Med. Chem. Lett.* **2012**, *3* (5), 383–386.

(47) Davis, M. I.; Hunt, J. P.; Herrgard, S.; Ciceri, P.; Wodicka, L. M.; Pallares, G.; Hocker, M.; Treiber, D. K.; Zarrinkar, P. P. Comprehensive Analysis of Kinase Inhibitor Selectivity. *Nat. Biotechnol.* **2011**, *29* (11), 1046–1051.

(48) Gallagher, T. F.; Seibel, G. L.; Kassis, S.; Laydon, J. T.; Blumenthal, M. J.; Lee, J. C.; Lee, D.; Boehm, J. C.; Fier-Thompson, S. M.; Abt, J. W.; Soreson, M. E.; Smietana, J. M.; Hall, R. F.; Garigipati, R. S.; Bender, P. E.; Erhard, K. F.; Krog, A. J.; Hofmann, G. A.; Sheldrake, P. L.; McDonnell, P. C.; Kumar, S.; Young, P. R.; Adams, J. L. Regulation of Stress-Induced Cytokine Production by Pyridinylimidazoles; Inhibition of CSBP Kinase.

Bioorg. Med. Chem. **1997**, *5* (1), 49–64.

(49) Carlino, L.; Rastelli, G. Dual Kinase-Bromodomain Inhibitors in Anticancer Drug Discovery: A Structural and Pharmacological Perspective. *J. Med. Chem.* **2016**, *59* (20), 9305–9320.

(50) Andrews, F. H.; Singh, A. R.; Joshi, S.; Smith, C. A.; Morales, G. A.; Garlich, J. R.; Durden, D. L.; Kutateladze, T. G. Dual-Activity PI3K–BRD4 Inhibitor for the Orthogonal Inhibition of MYC to Block Tumor Growth and Metastasis. *Proc. Natl. Acad. Sci.* **2017**, *114* (7), E1072–E1080.

(51) Adams, J. L.; Sheldrake, P. W.; Gallagher, T. F.; Garigipati, R. Novel 1,4,5-Substituted Imidazole Compounds and Compositions for Use in Therapy as Cytokine Inhibitors. US5593992 A, 1995.

(52) Ryzhakov, D.; Jarret, M.; Guillot, R.; Kouklovsky, C.; Vincent, G. Radical-Mediated Dearomatization of Indoles with Sulfinate Reagents for the Synthesis of Fluorinated Spirocyclic Indolines. *Org. Lett.* **2017**, *19* (23), 6336–6339.

(53) Chan, K.; Erdman, P. E.; Fung, L.; Mercurio, F.; Sullivan, R.; Torres, E. Compounds Targeting Proteins, Compositions, Methods, and Uses Thereof. US Patent 20180170948, 2017.

(54) Erijman, A.; Dantes, A.; Bernheim, R.; Shifman, J. M.; Peleg, Y. Transfer-PCR (TPCR): A Highway for DNA Cloning and Protein Engineering. *J. Struct. Biol.* **2011**, *175* (2), 171–177.

(55) Kabsch, W. XDS. *Acta Crystallogr D Biol Crystallogr* **2010**, *66* (Pt 2), 125–132.

(56) Adams, P. D.; Afonine, P. V.; Bunkóczi, G.; Chen, V. B.; Davis, I. W.; Echols, N.; Headd, J. J.; Hung, L. W.; Kapral, G. J.; Grosse-Kunstleve, R. W.; McCoy, A. J.; Moriarty, N. W.; Oeffner, R.; Read, R. J.; Richardson, D. C.; Richardson, J. S.; Terwilliger, T. C.; Zwart, P. H. PHENIX: A Comprehensive Python-Based System for Macromolecular Structure Solution. *Acta Crystallogr. Sect. D Biol. Crystallogr.* **2010**, *66* (2), 213–221.

(57) Emsley, P.; Lohkamp, B.; Scott, W. G.; Cowtan, K. Features and Development of Coot. *Acta Crystallogr. Sect. D Biol. Crystallogr.* **2010**, *66* (4), 486–501.

(58) Hexum, J. K.; Tello-Aburto, R.; Struntz, N. B.; Harned, A. M.; Harki, D. A. Bicyclic Cyclohexenones as Inhibitors of NF-κB Signaling. *ACS Med. Chem. Lett.* **2012**, *3* (6), 459–464.

Table of Contents Graphic

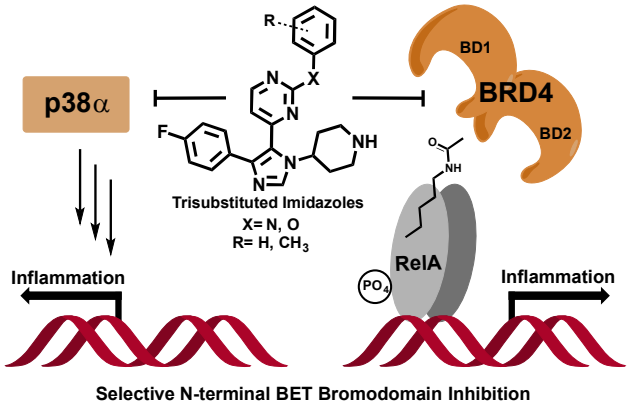

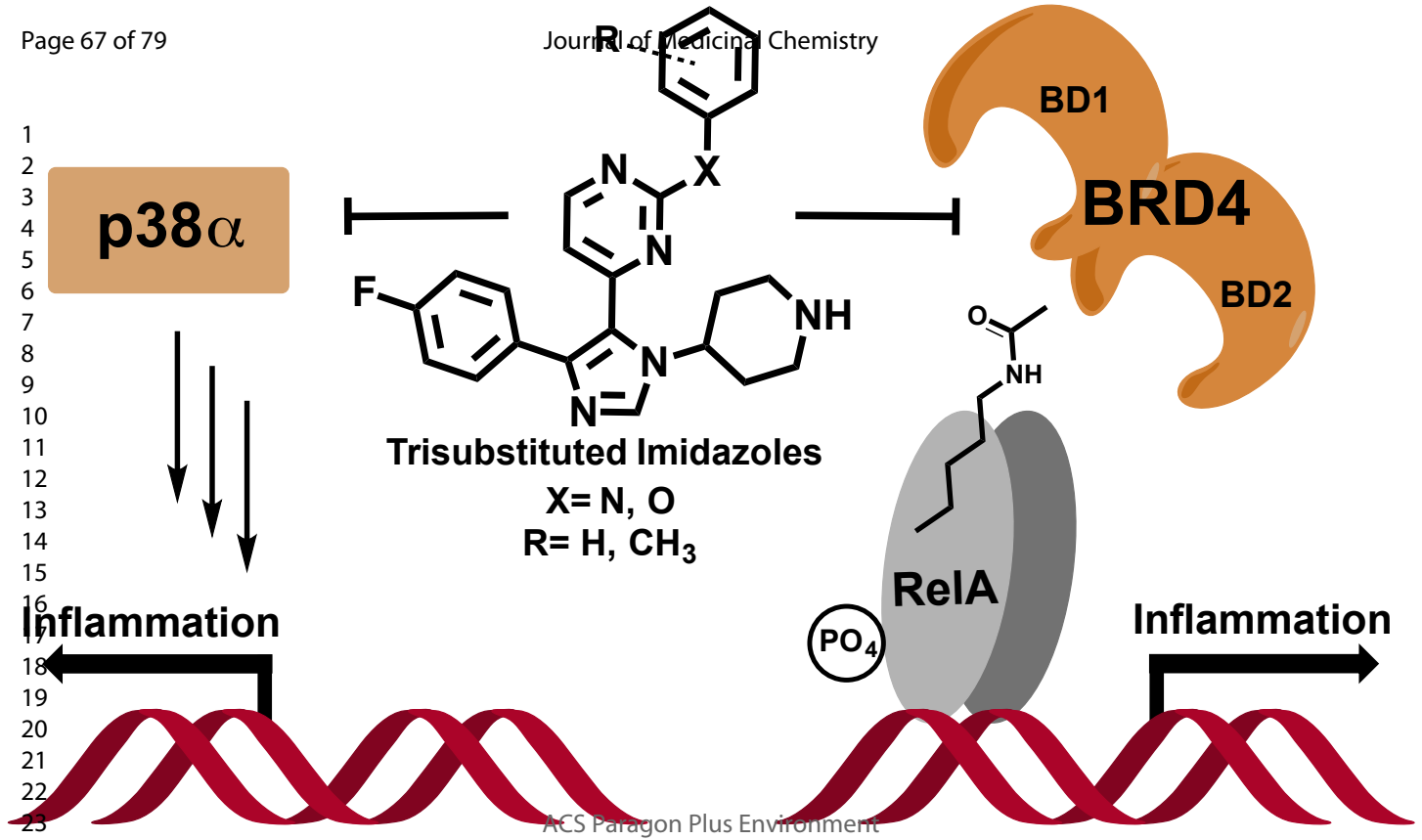

Selective N-terminal BET Bromodomain Inhibition

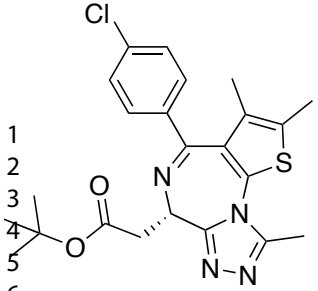

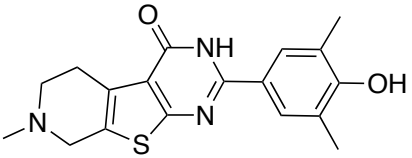

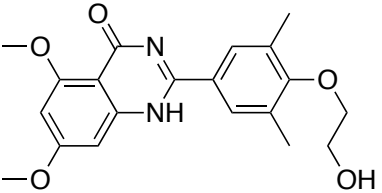

Many Pan-BET Inhibitors

(+)-JQ1 (1)
BRD4(1) K_d = 0.049 μM
BRD4(2) K_d = 0.090 μM
BRD3(1) K_d = 0.059 μM
BRD3(2) K_d = 0.082 μM
BRD2(1) K_d = 0.13 μM
BRD2(2) K_d = ND

BRD4 Inhibitors

FL-411 (2)
BRD4(1) IC_{50} = 0.47 μM
BRD4(2) IC_{50} = 0.93 μM
BRD3(1) IC_{50} = >100 μM
BRD3(2) IC_{50} = >100 μM
BRD2(1) IC_{50} = 24.6 μM
BRD2(2) IC_{50} = >100 μM

BET-D2 Inhibitors

RVX-208 (3)
BRD4(1) K_d = 1.1 μM
BRD4(2) K_d = 0.13 μM
BRD3(1) K_d = 4.0 μM
BRD3(2) K_d = 0.19 μM
BRD2(1) K_d = 5.8 μM
BRD2(2) K_d = 0.25 μM

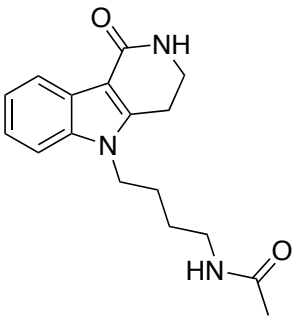

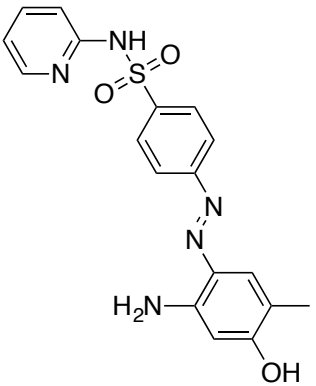

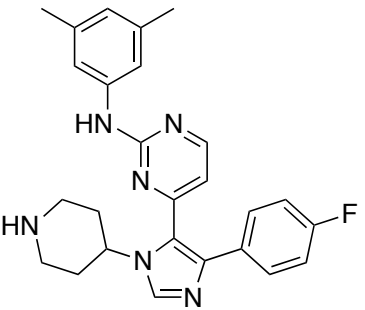

Few BET-D1 Inhibitors

Quinone (4)
BRD4(1) K_d = 3.4 μM
BRD4(2) K_d = >75 μM
BRD3(1) K_d = 3.7 μM
BRD3(2) K_d = >75 μM
BRD2(1) K_d = 8.6 μM
BRD2(2) K_d = >75 μM

MS-436 (5)
BRD4(1) K_i = < 0.085 μM
BRD4(2) K_i = 0.34 μM
BRD3(1) K_i = 0.10 μM
BRD3(2) K_i = 0.14 μM

This Work:

Compound V
BRD4(1) IC_{50} = 1.8 μM,
K_d = 1.2 μM
BRD4(2) IC_{50} = >100 μM
BRD3(1) IC_{50} = 11 μM
BRD3(2) IC_{50} = >100 μM
BRD2(1) IC_{50} = 29 μM
BRD2(2) IC_{50} = 67 μM

A

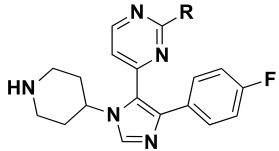

R =		IC$_{50}$ by FP (μM)			
		BRDT(1)	BRD4(1)	BRDT(2)	BRD4(2)
I		18 ± 0.5	3.7 ± 1	>250	ND
II	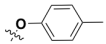	88 ± 8	24 ± 0.8	>250	ND
III	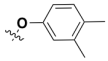	13 ± 3	2.9 ± 0.2	>250	ND
IV	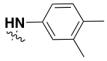	4.7 ± 1.0*	1.3 ± 0.2	>250	>250
V		3.5 ± 0.5*	1.7 ± 0.4	>250	>250
VI		>250	>250	>250	ND

B

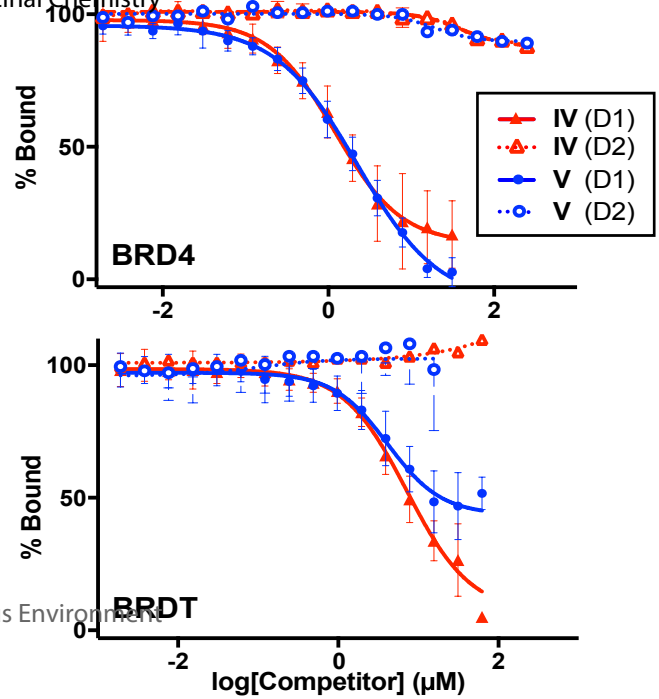

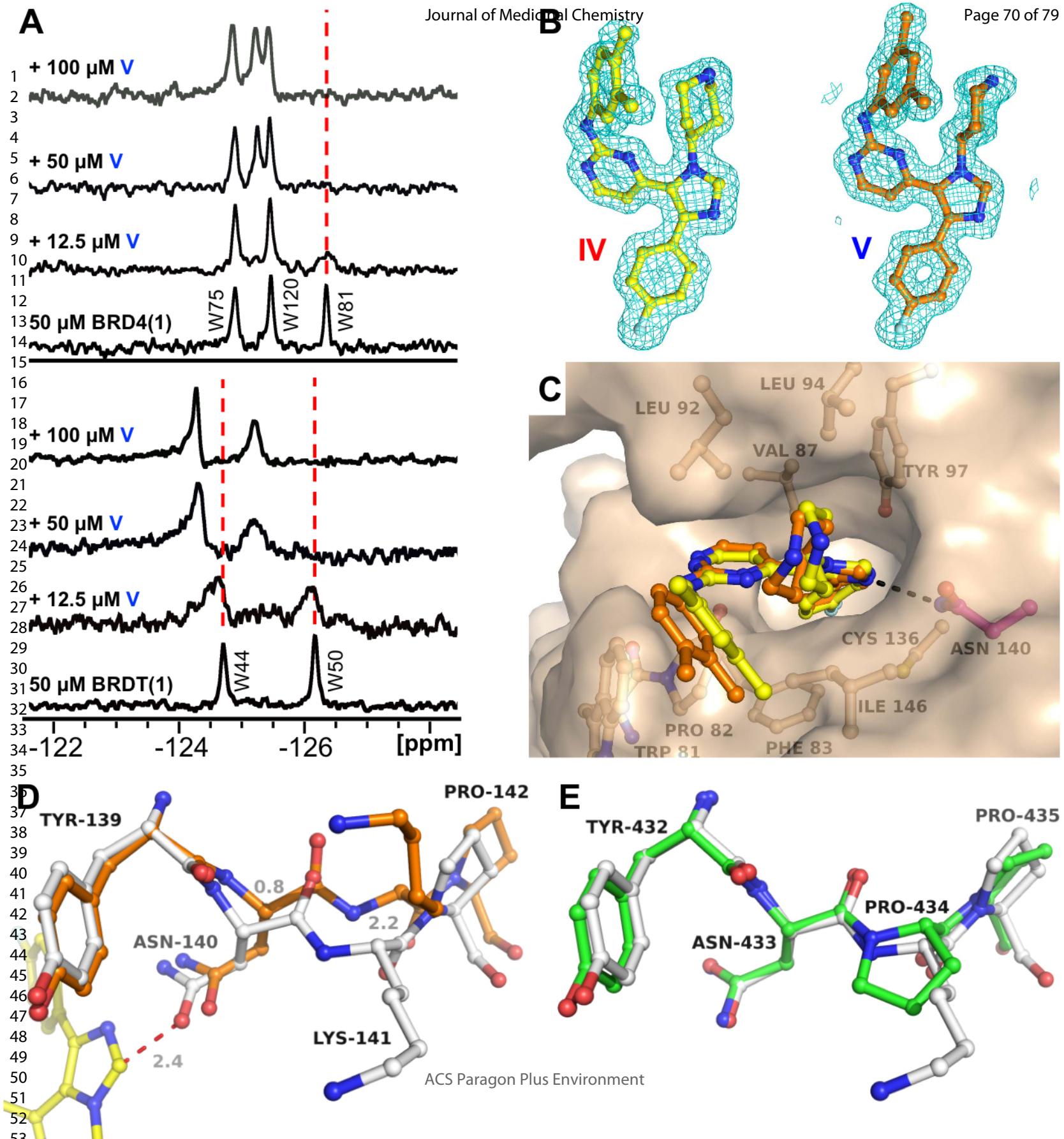
A
+ 100 μM V
+ 50 μM V
+ 12.5 μM V
50 μM BRD4(1)
W75
W120
W81
+ 100 μM V
+ 50 μM V
+ 12.5 μM V
50 μM BRDT(1)
W44
W50
-122
-124
-126
[ppm]
B
IV
V
C
LEU 94
LEU 92
VAL 87
TYR 97
CYS 136
ASN 140
ILE 146
PRO 82
TRP 81
PHE 83
D
TYR-139
PRO-142
0.8
2.2
ASN-140
LYS-141
2.4
E
TYR-432
PRO-435
PRO-434
ASN-433

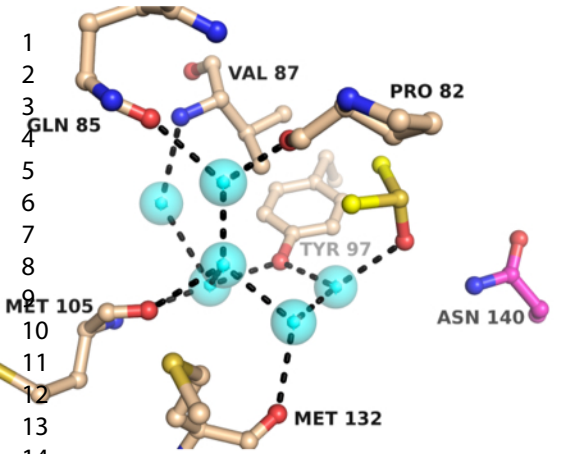

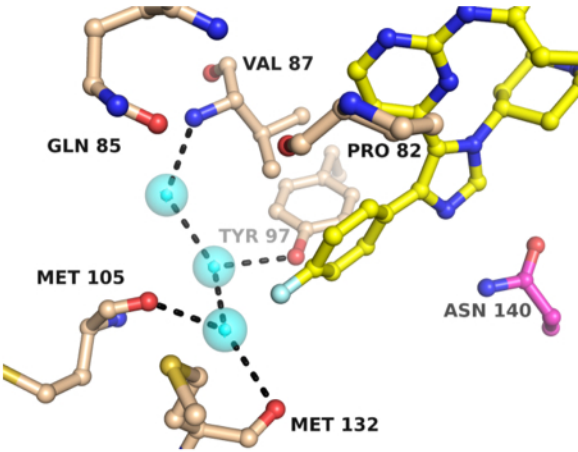

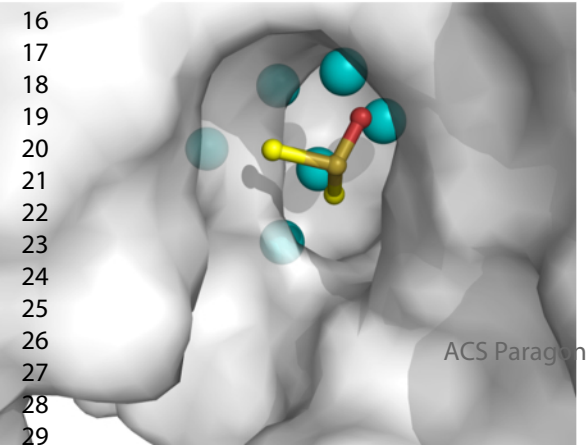

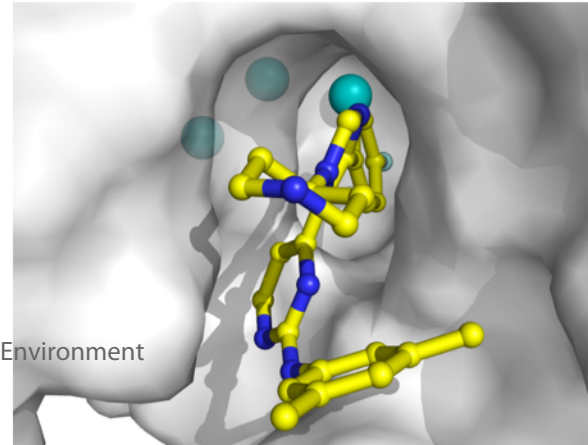

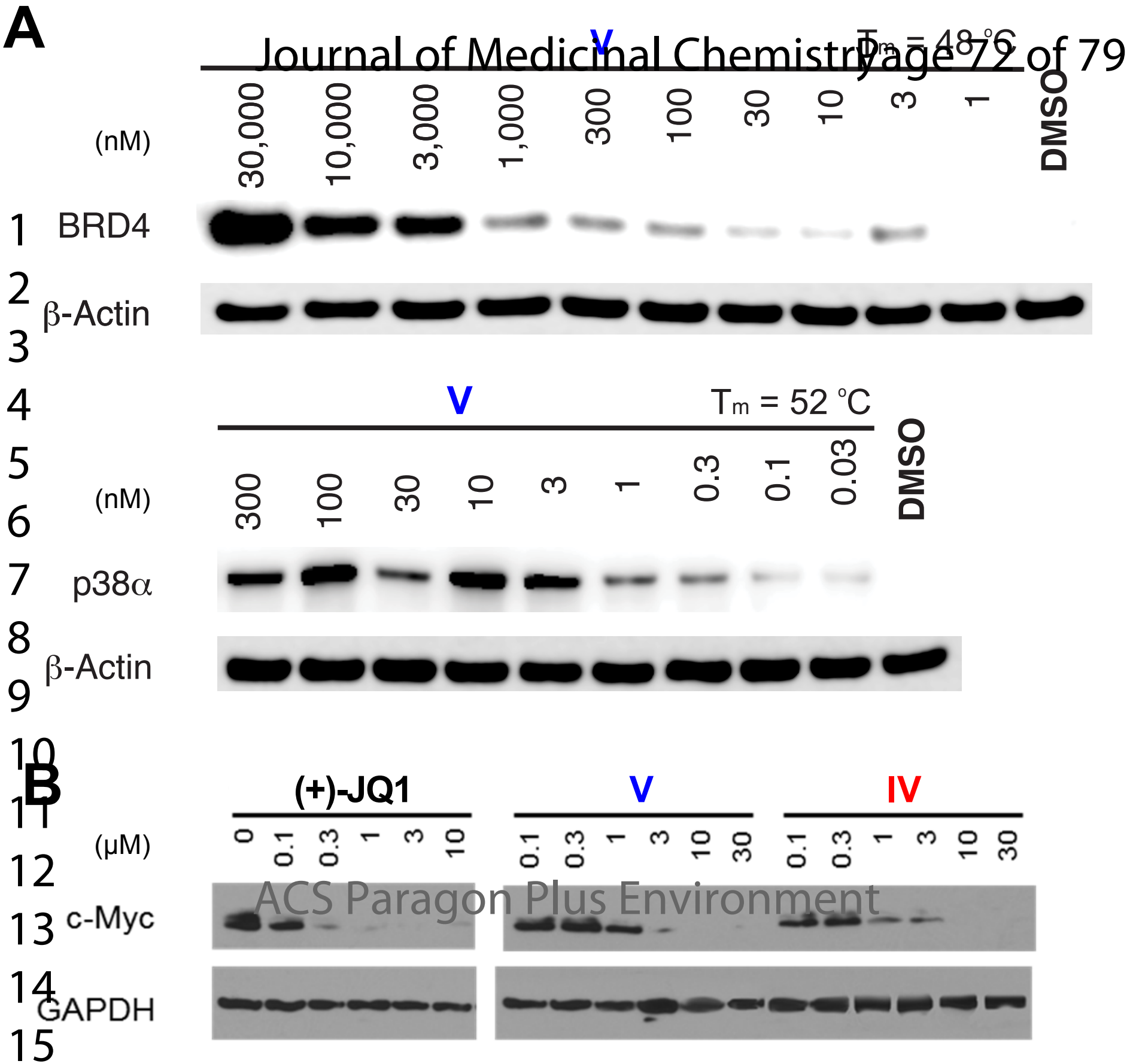

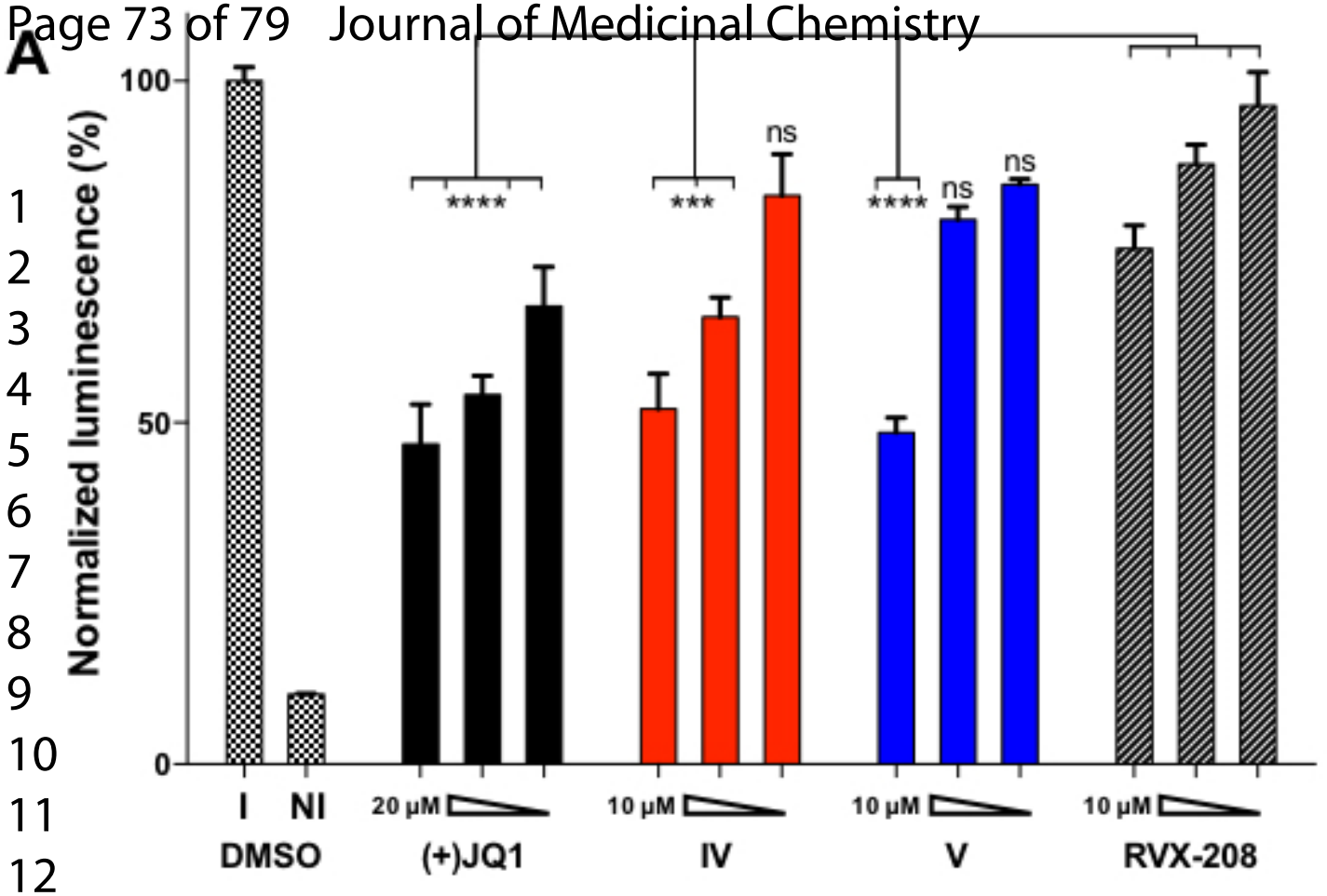

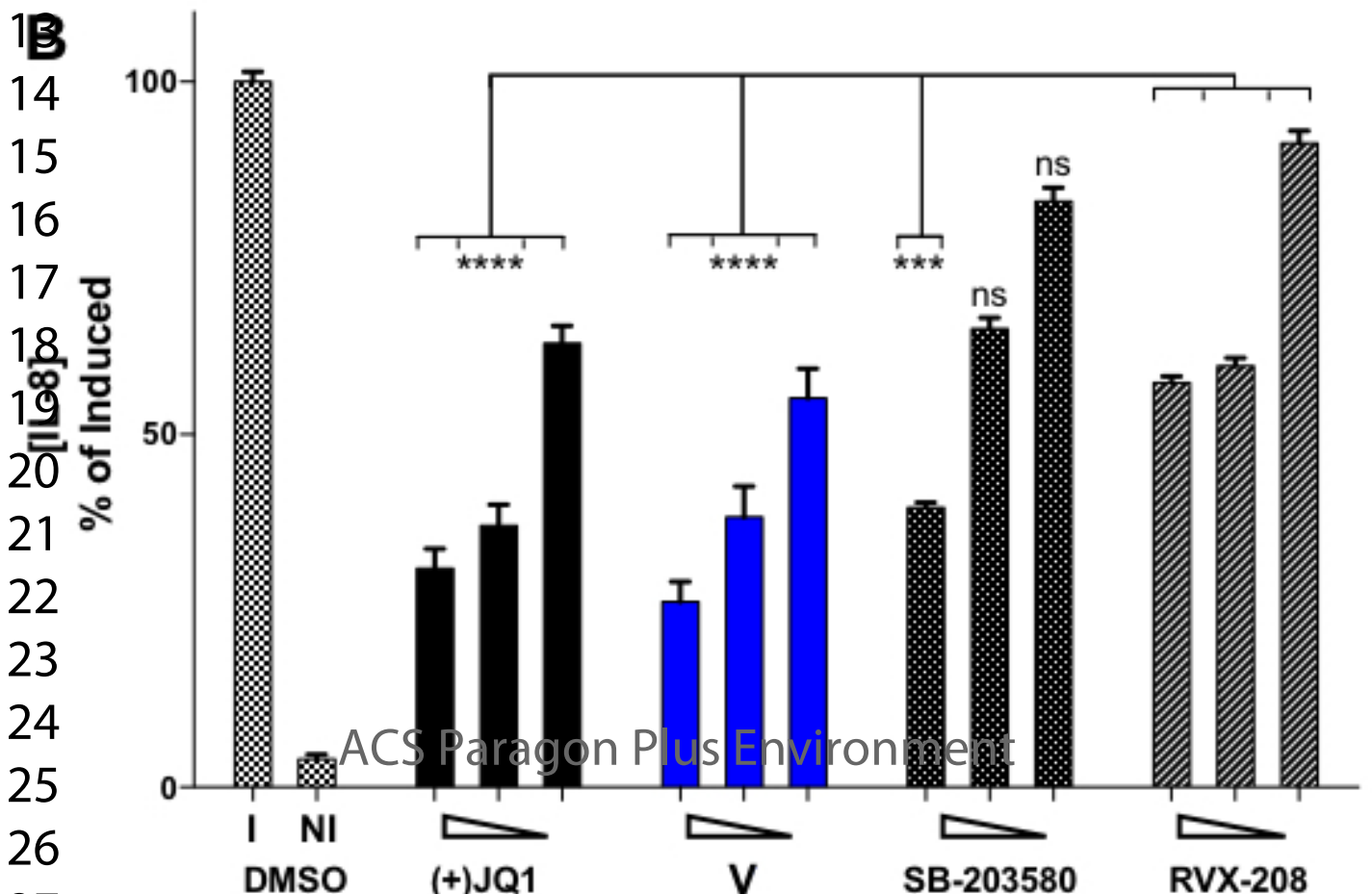

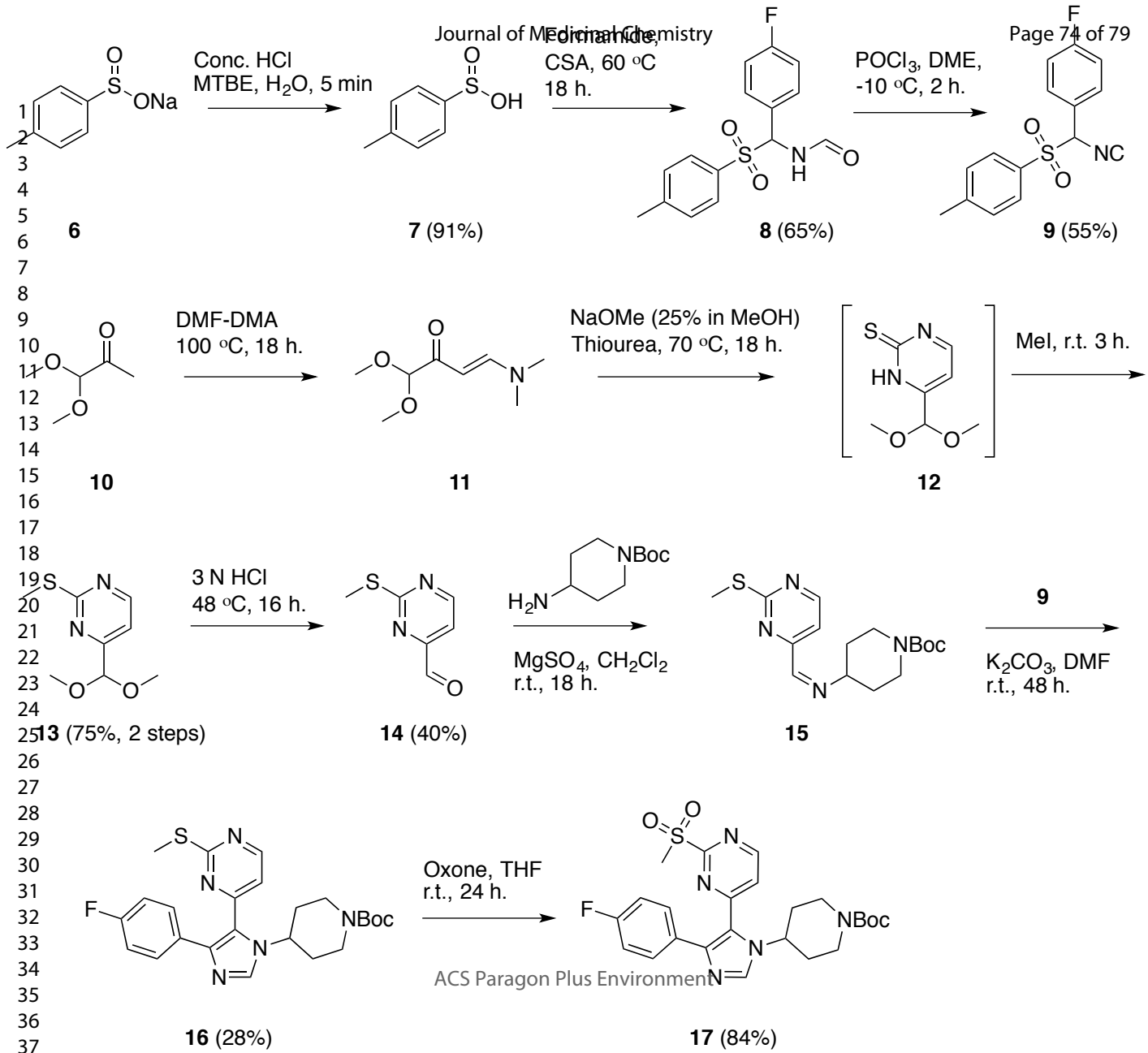

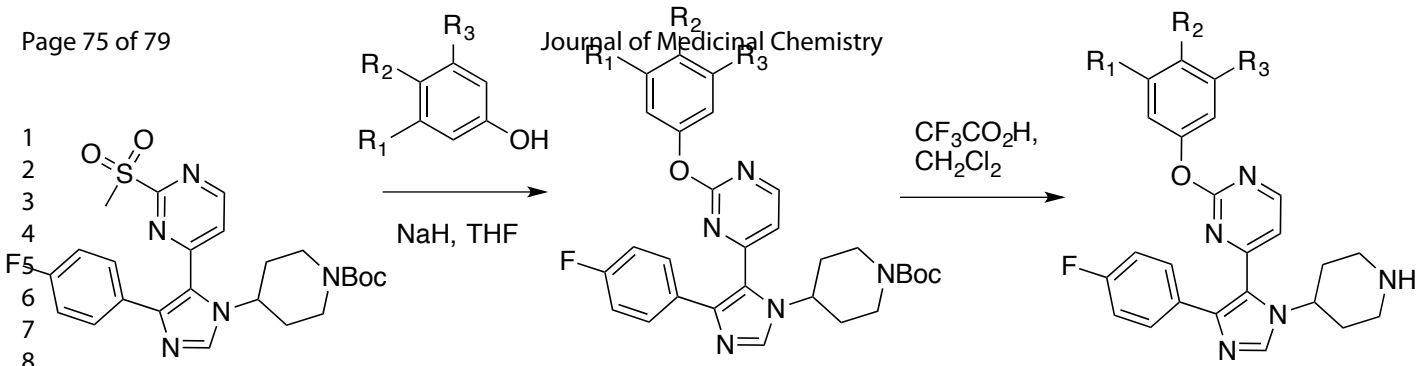

17

18 $R_{1,3} = CH_3$, $R_2 = H$ (59%)
19 $R_{1,3} = H$, $R_2 = CH_3$ (88%)
20 $R_{1,2} = CH_3$, $R_3 = H$ (95%)

I $R_{1,3} = CH_3$, $R_2 = H$ (70%)
II $R_{1,3} = H$, $R_2 = CH_3$ (50%)
III $R_{1,2} = CH_3$, $R_3 = H$ (52%)

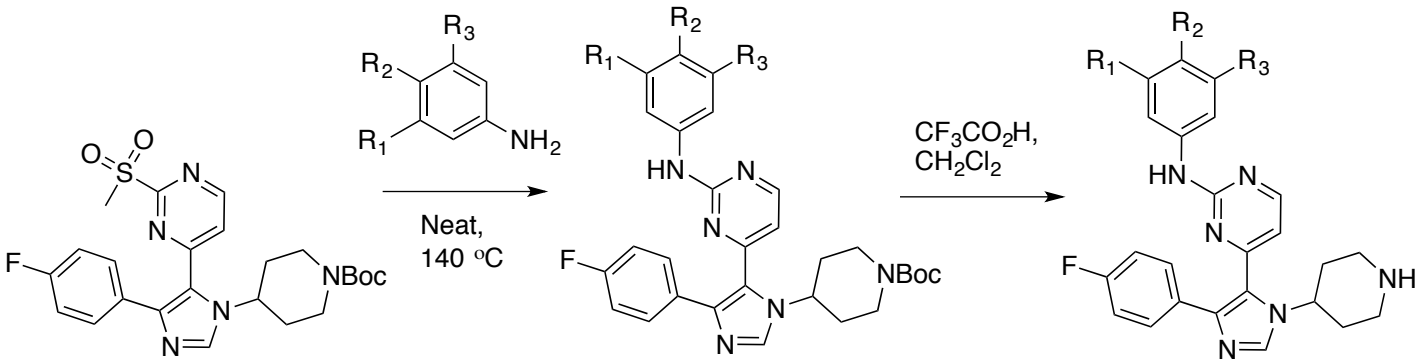

17

21 $R_{1,2} = CH_3$, $R_3 = H$ (46%)
22 $R_{1,3} = CH_3$, $R_2 = H$ (55%)

IV $R_{1,2} = CH_3$, $R_3 = H$ (50%)
V $R_{1,3} = CH_3$, $R_2 = H$ (96%)

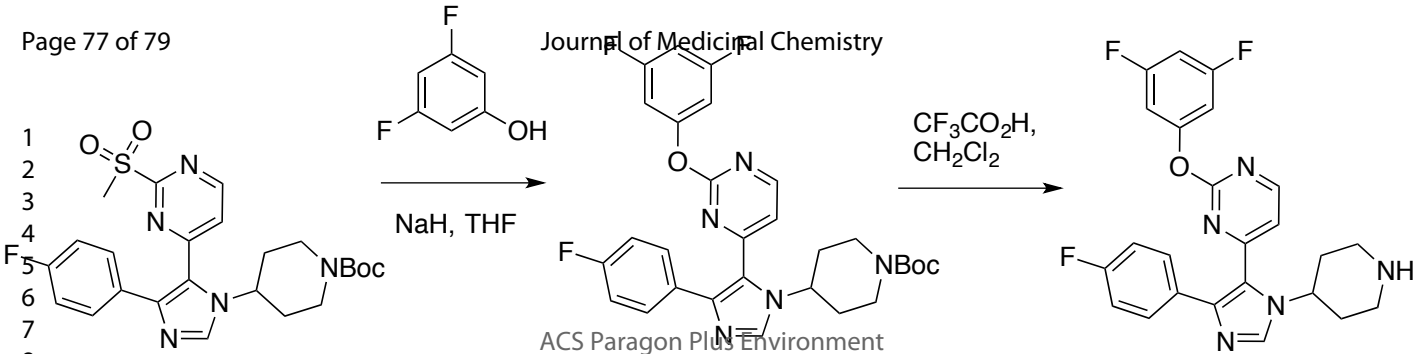

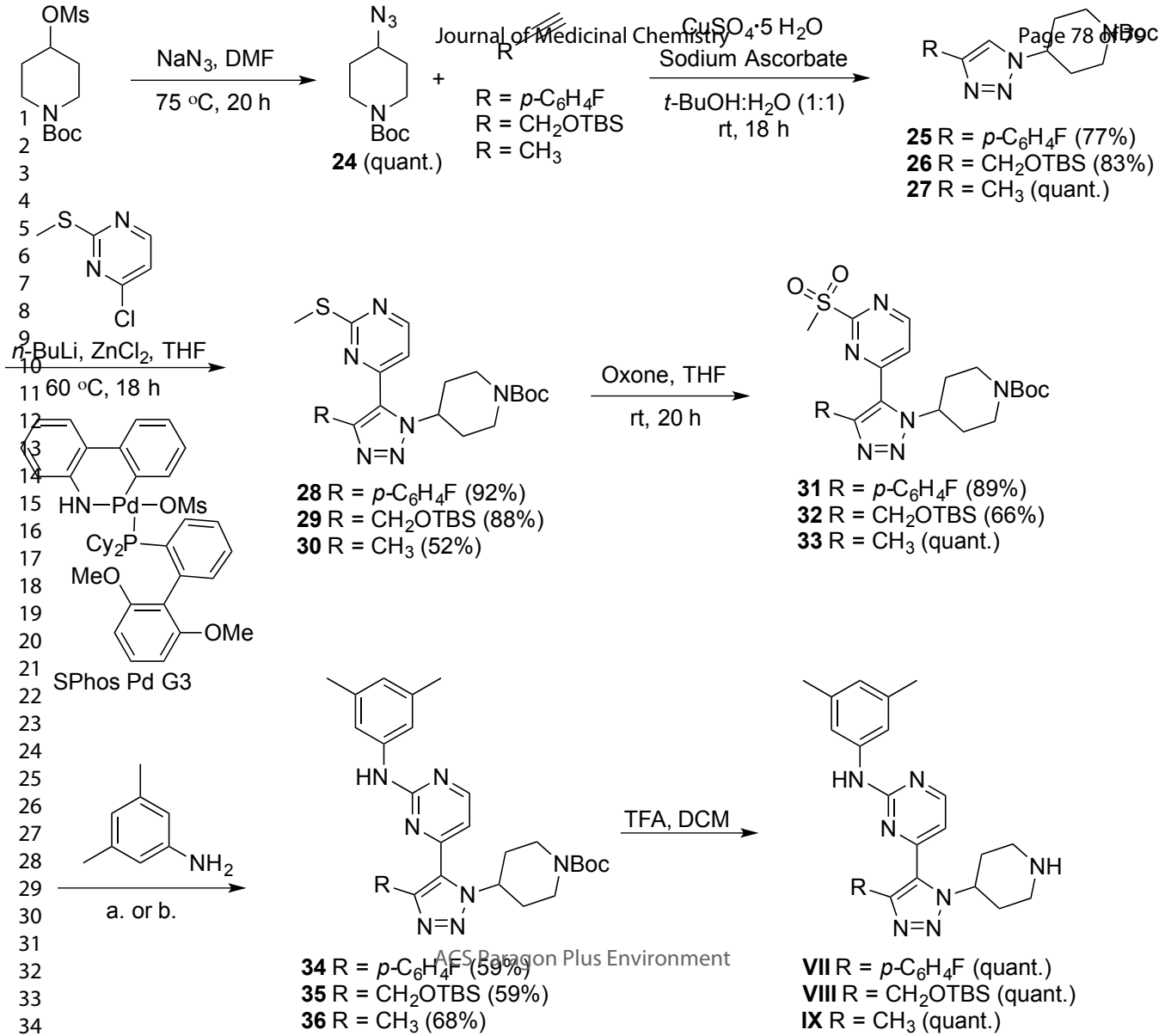
OMs
N
Boc
NaN3, DMF
75 °C, 20 h
N3
N
Boc
24 (quant.)
R
R = p-C6H4F
R = CH2OTBS
R = CH3
CuSO4·5 H2O
Sodium Ascorbate
t-BuOH:H2O (1:1)
rt, 18 h
R
N
N=N
NBoc
25 R = p-C6H4F (77%)
26 R = CH2OTBS (83%)
27 R = CH3 (quant.)
S
N
N
Cl
n-BuLi, ZnCl2, THF
60 °C, 18 h
HN—Pd—OMs
Cy2P
MeO
OMe
SPhos Pd G3
28 R = p-C6H4F (92%)
29 R = CH2OTBS (88%)
30 R = CH3 (52%)
Oxone, THF
rt, 20 h
O
S
O
31 R = p-C6H4F (89%)
32 R = CH2OTBS (66%)
33 R = CH3 (quant.)
NH2
a. or b.
HN
34 R = p-C6H4F (59%)
35 R = CH2OTBS (59%)
36 R = CH3 (68%)
TFA, DCM
NH
VII R = p-C6H4F (quant.)
VIII R = CH2OTBS (quant.)
IX R = CH3 (quant.)

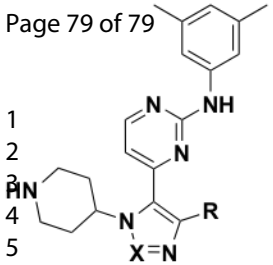

	R	X	IC_{50} by ALPHAScreen (μM)						
			BRD4		BRD3		BRD2		BRDT
			D1	D2	D1	D2	D1	D2	D1
V	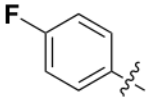	C	1.8	>100	11.2	>100	29	67	5.3
VII	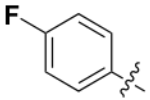	N	27	75	51	110	43	30	36
VIII	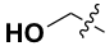	N	160	102	200	310	>250	260	110
IX		N	1.3	0.56	0.77	2.4	1.8	12	1.6